Journal of Medicinal Chemistry

pubs.acs.org/jmc

Article

Discovery of Selective Small-Molecule Inhibitors for the ENL YEATS Domain

Xinyu R. Ma,△ Longxia Xu,△ Shiqing Xu, Brianna J. Klein, Hongkuan Wang, Sukant Das, Kuai Li, Kai S. Yang, Sana Sohail, Andrew Chapman, Tatiana G. Kutateladze, Xiaobing Shi, Wenshe Ray Liu,* and Hong Wen*

Cite This: https://doi.org/10.1021/acs.jmedchem.1c00367

Read Online

ACCESS | Metrics & More | Article Recommendations | Supporting Information

ABSTRACT: Eleven-nineteen leukemia (ENL) protein is a histone acetylation reader essential for disease maintenance in acute leukemias, in particular, the *mixed-lineage leukemia* (*MLL*)-rearranged leukemia. In this study, we carried out high-throughput screening of a small-molecule library to identify inhibitors for the ENL YEATS domain. Structure−activity relationship studies of the hits and structure-based inhibitor design led to two compounds, **11** and **24**, with IC_{50} values below 100 nM in inhibiting the ENL−acetyl-H3 interaction. Both compounds, and their precursor compound **7**, displayed strong selectivity toward the ENL YEATS domain over all other human YEATS domains. Moreover, **7** exhibited on-target inhibition of ENL in cultured cells and a synergistic effect with the bromodomain and extraterminal domain inhibitor JQ1 in killing leukemia cells. Together, we have developed selective chemical probes for the ENL YEATS domain, providing the basis for further medicinal chemistry-based optimization to advance both basic and translational research of ENL.

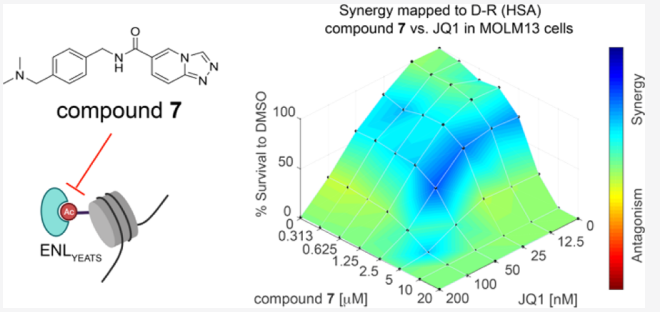

INTRODUCTION

Post-translational modifications of histones play an important role in the epigenetic regulation of gene expression. These modifications serve as binding sites to recruit reader proteins, which in turn transduce the epigenetic signals into downstream functional outcomes.[1,2] In addition to small compounds that modulate enzymatic activities of the histone-modifying enzymes, perturbations of reader−histone interactions also provide attractive therapeutic potentials. One such example is the BET bromodomain inhibitor.[3,4] Bromodomains are known as readers of histone acetylation.[5] Recent studies from our laboratories and others have identified the YEATS domains as a new family of epigenetic readers that bind to not only histone acetylation but also other types of acylations such as crotonylation.[6−16]

The YEATS domain, named after its five founding members (Yaf9, ENL, AF9, Taf14, and Sas5), is evolutionarily conserved from yeast to humans.[17] The human genome encodes four YEATS domain-containing proteins ENL, AF9, YEATS2, and GAS41 that all associate with chromatin-associated protein complexes.[18,19] ENL and AF9 are paralogues that share a similar protein structure including a highly conserved YEATS domain. Both ENL and AF9 are subunits of the super elongation complex and the complex of the histone H3K79 methyltransferase DOT1L, but mutually exclusive.[20,21] We and others previously showed that ENL, but not AF9, is required for disease maintenance in acute leukemias, in particular, the *mixed-lineage leukemia* (*MLL*)-rearranged leukemia.[14,22] Depletion of ENL or disrupting the interaction between its YEATS domain and acetylated histones suppresses leukemia progression. In addition, hotspot ENL YEATS domain mutations were found in Wilms' tumor patients.[23,24] We showed that the reader function of the ENL YEATS domain is indispensable for the gain-of-function mutations in the oncogenesis of Wilms' tumor.[25] Together, all these studies suggest that the YEATS domain of ENL is an attractive therapeutic target.

The acetyllysine-binding pocket of the ENL YEATS domain is a long and narrow hydrophobic channel, making it a potentially good target for developing small-molecule inhibitors.[14] Indeed, recent publications of acetyllysine competitive small compounds and peptide-mimic chemical probes demonstrate that the ENL YEATS domain is pharmacologically tractable.[26−32] The peptide-mimic chemical probes showed slightly higher potency to the ENL YEATS domain

Received: February 28, 2021

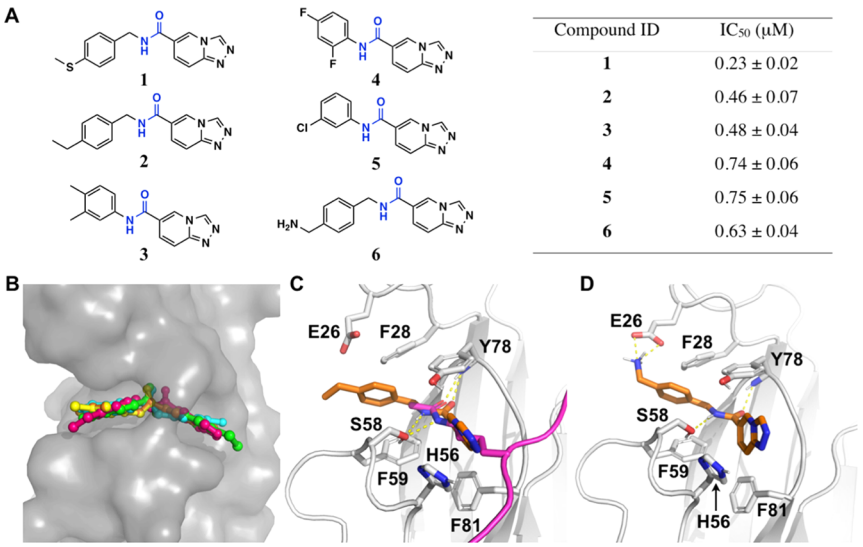

Figure 1. Structural modeling of the five initial HTS hits, **1**−**5**, and an amine analogue **6** with the ENL YEATS domain. (A) Chemical structures of compounds **1**−**6** (left) and their IC_{50} values in inhibiting the His-ENL−H3K9ac interaction in the AlphaScreen assay (right). (B) Structural model showing binding of **1**−**5** to the ENL YEATS domain. Modeling was based on the crystal structure of the ENL YEATS domain (PDB entry: 5J9S). **1**−**5** are shown in stick representation, and the ENL YEATS domain is shown in a contoured surface structure. Atoms in ENL are colored in gray, compound **1** in green, **2** in hot pink, **3** in yellow, **4** in cyan, and **5** in orange. (C) Modeled interaction of **2** with ENL. The Cα atoms of **2** are colored in orange and two hydrogen bonds (dashed lines) to S58 and Y78 of ENL are colored in yellow. Acetyllysine in the H3K27ac ligand in the original crystal structure is colored in hot pink and its two hydrogen bonds with E58 and Y78 are shown for comparison. (D) Modeled interaction of **6** with ENL. The Cα atoms of **6** are colored in orange. The amine in **6** shows a salt-bridge interaction with E26 in ENL.

than other YEATS domains, largely due to interactions outside of the acetyllysine binding pocket.[30] In contrast, the small molecule ENL inhibitors reported so far failed to distinguish ENL from its close paralogue AF9. In addition, none of these small-molecule compounds showed significant impact on ENL-dependent leukemia cell growth, suggesting that development of potent, selective ENL YEATS-domain inhibitors is in great need. Here, we report the discovery of small-molecule compounds that exhibit preferential binding to ENL compared to AF9 and other YEATS-domain proteins. Two compounds, **11** and **24**, displayed IC_{50} values below 100 nM in inhibiting the ENL−acetyl-H3 interaction *in vitro*. In leukemia cells, compound **7** reduced ENL target gene expression and suppressed leukemia cell growth. In addition, **7** exhibited a synergistic effect with the BET bromodomain inhibitor JQ1 in killing leukemia cells. Our study provided valuable selective ENL chemical probes and potential leads for further medicinal chemistry-based optimization to advance both basic and translational research of ENL.

RESULTS

High-Throughput Library Screen for ENL YEATS-Domain Inhibitors. In order to identify small-molecule inhibitors for the YEATS domain of ENL, we first established an AlphaScreen assay system for high-throughput screening (HTS) of small-molecule compounds. In this assay system, two analytes, a 6× His-tagged ENL YEATS domain (His-ENL) and a biotin-H3K9ac peptide (histone H3 residues 1−21 with an acetylation at Lys 9) were immobilized on PerkinElmer Ni^{2+}-chelating acceptor and streptavidin donor beads, respectively (Supporting Information, Figure S1A). Protein and peptide dose−response assays determined optimal concentrations of His-ENL and biotin-H3K9ac to be 100 and 30 nM, respectively (Supporting Information, Figures S1B,C). We also determined the optimized beads concentration to be 10 μg/mL. This assay system was further evaluated in a high-throughput setting in 384-well plates. Interplate variations were measured between two separate plates and on two separate days, yielding robust and highly reproducible results with a high signal/background (S/B) ratio (39.02), low coefficient of variation (3.5%), and an excellent Z' factor (0.92) (Supporting Information, Figure S1D). Dimethyl sulfoxide (DMSO) tolerance of the assay (0.1−1%) indicated that the AlphaScreen signals were maintained at 95 and 85% in the presence of 0.1 and 0.5% DMSO, respectively. We also set up a counter assay using a biotin-14× His peptide to eliminate compounds that interfere with AlphaScreen assay components. Together, these data demonstrate that the AlphaScreen assay we developed is suitable for HTS of ENL inhibitors, with superior sensitivity and reproducibility.

After adapting the AlphaScreen-based HTS system to an automated format for ENL (100 nM His-ENL, 10 nM biotin-H3K9ac, 0.1% DMSO, and 2.5 μg/mL AlphaScreen beads), we proceeded to screen a small-molecule library of 66,625 compounds with diverse chemical scaffolds. Nonfragment compounds were screened at a concentration of 10 μM, and fragment-based compounds were screened at a concentration of 50 μM. In the primary screen, we obtained 4648 hits with above 50% inhibition. Confirmation and counter assays yielded 524 compounds with above 60% inhibition of the His-ENL−H3K9ac interaction and below 20% inhibition of the counter screen. We then subjected the top 100 compounds to full dose−response curve validation and obtained 37 compounds with IC_{50} values below 5 μM, including 8 compounds with IC_{50} below 1 μM (Supporting Information, Table S1).

Structure-Based Inhibitor Design and Structure−Activity Relationship Studies. Among the top eight hits that have an IC_{50} value below 1 μM (Supporting Information, Table S1), five, named as **1**−**5**, are structurally similar and share a same pharmacophore [1,2,4]triazolo[4,3-*a*]pyridine-6-

https://doi.org/10.1021/acs.jmedchem.1c00367
J. Med. Chem. XXXX, XXX, XXX−XXX

Scheme 1. Synthesis of Compounds 6−19

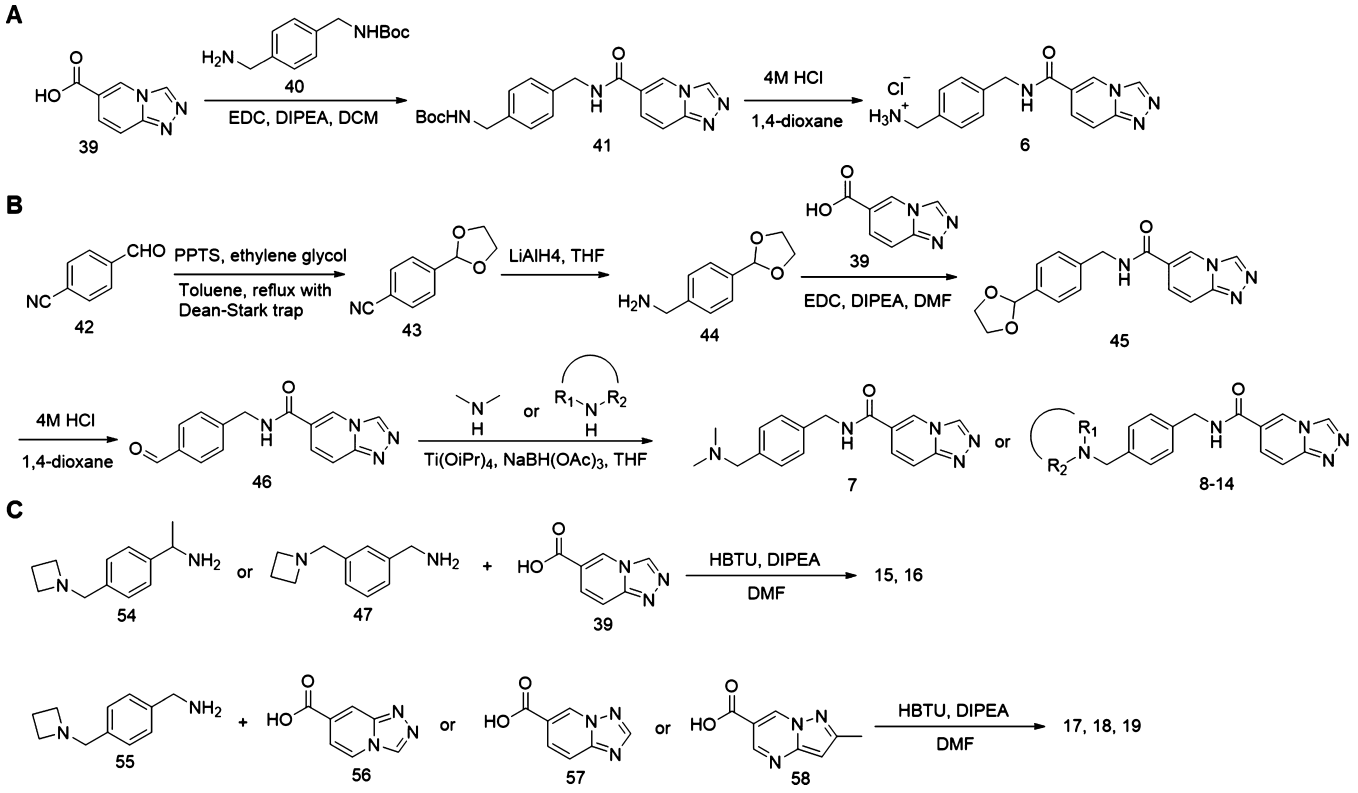

Table 1. Chemical Structures and IC_{50} Values of 7−28

ID	Structure	IC_{50} (nM)	ID	Structure	IC_{50} (nM)
7	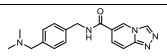	621 ± 40	18	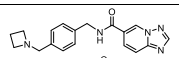	> 5000
8	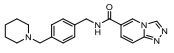	636 ± 64	19	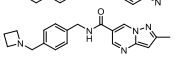	> 5000
9	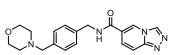	891 ± 91	20	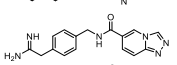	2,015 ± 92
10	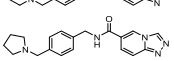	379 ± 27	21	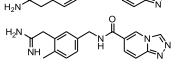	2,016 ± 120
11	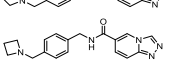	51 ± 2.9	22	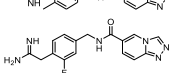	1,270 ± 39
12	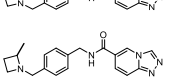	185 ± 10	23	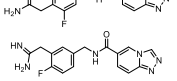	1,156 ± 57
13		266 ± 13	24	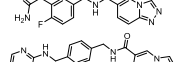	85 ± 5.5
14	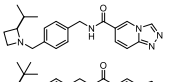	264 ± 21	25	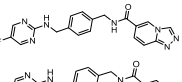	> 1,000
15	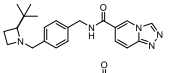	202 ± 5.8	26	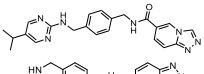	417 ± 22
16	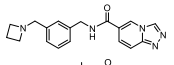	> 1,000	27	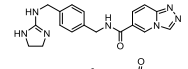	> 5,000
17	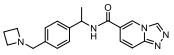	> 5,000	28	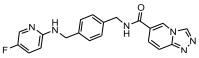	> 2,000

amide, suggesting a preferential binding of this pharmacophore to the ENL YEATS domain (Figure 1A and Supporting Information, Figure S2). All these five compounds also contain an aryl substituent at the amide nitrogen side, allowing them to be generally defined as *N*,*C*-diarylamides. To understand how these compounds interact with ENL, we performed docking analysis using an existing crystal structure of the ENL YEATS domain (the PDB entry: 5J9S). The results showed that all five compounds fit nicely to the acetyllysine binding channel of ENL (Figure 1B). The compounds are bound to the ENL YEATS domain with a similar orientation as an acetyllysine in a native histone ligand. Similar to the acetyllysine side chain amide, the amide in **1**−**5** is poised to form two hydrogen bonds with S58 and Y78. Although the two aromatic rings can flip to bind either side of the channel, both potentially form π-stacking and van der Waals interactions with residues F28, H56, F59, Y78, and F81 in ENL for preferential binding

https://doi.org/10.1021/acs.jmedchem.1c00367
J. Med. Chem. XXXX, XXX, XXX−XXX

Scheme 2. Synthesis of Compounds 20−28

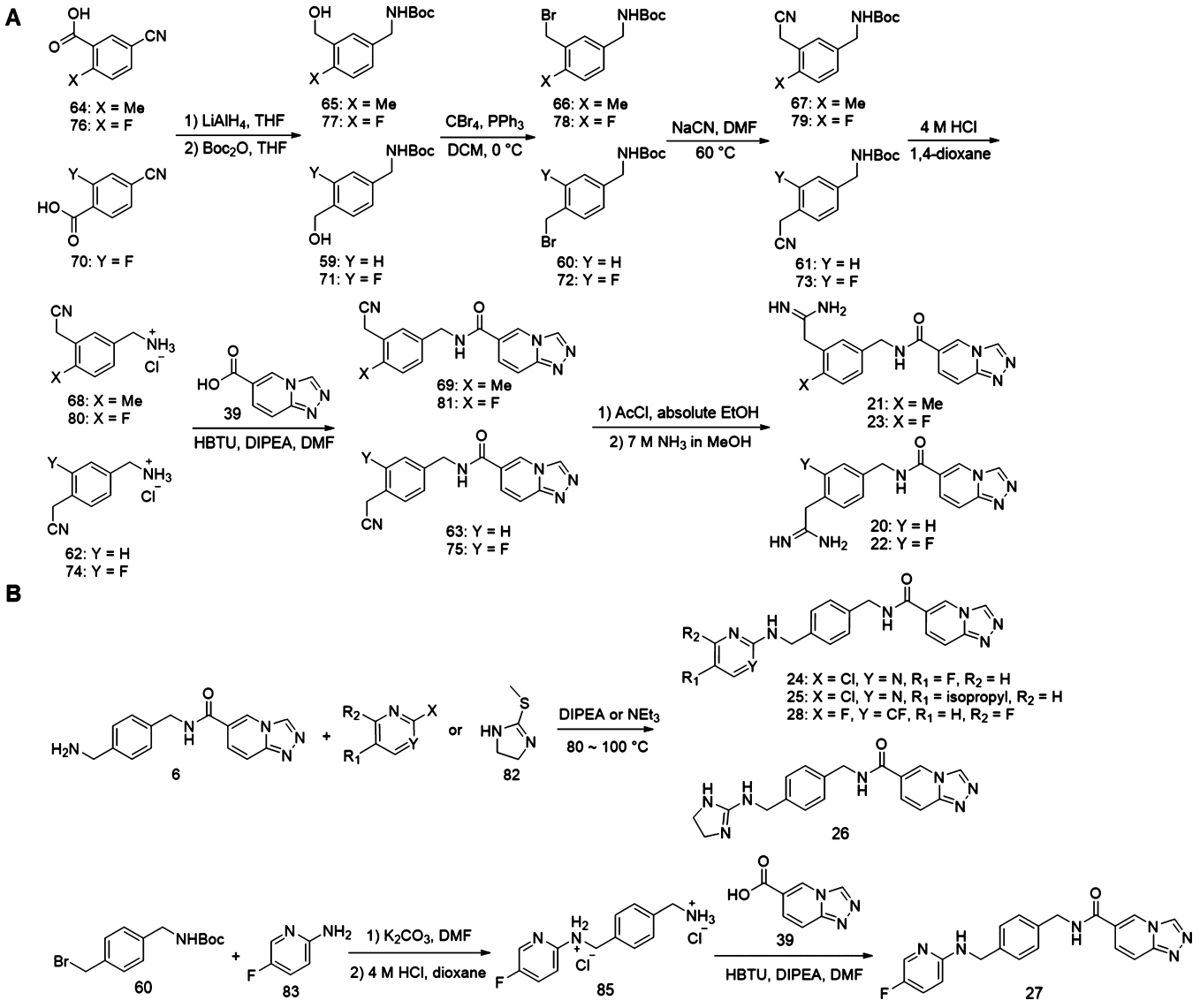

(Figure 1C). The modeling analysis also indicated that **1**−**5** occupy almost fully the acetyllysine binding channel of ENL.

Since ENL has relatively flat interfaces on the two sides of the acetyllysine binding channel, there is a little space for chemical maneuvers of **1**−**5** for improved binding. However, we noticed that E26, a residue at the edge of the acetyllysine binding channel can potentially flip its side chain toward the acetyllysine binding channel to interact with a ligand such as **2** (Figure 1C). We deemed that by adding a positively charged amine or amidine to **2**, it is possible that a salt-bridge interaction with E26 can be introduced for strong binding to ENL. Therefore, we synthesized compound **6** (Scheme 1A) and tested its inhibition of the interaction between His-ENL and biotin-H3K9ac. The determined IC_{50} value for **6** was 0.63 μM, which is similar to that for **2** (Figure 1A and Supporting Information, Figure S2). Since the introduction of an amine makes the compound more favorable to dissolve in water, the salt-bridge interaction may compensate the energy loss due to desolvation when **6** binds ENL, resulting in no improvement. Indeed, in the modeled structure, **6** interacts with ENL similar to **2** except that it engages E26 for a salt-bridge interaction (Figure 1D). We have also attempted to cocrystalize ENL with **6** for crystal structure determination, but unfortunately, it has not been successful.

Encouraged by the results from **6**, we expanded the scope of substitution groups on both sides of the amide bond of hit compounds for a comprehensive structure−activity relationship (SAR) study. A major focus was to maintain a positive charged amine, amidine, or guanidine as in **6** but tune the ENL binding as well as lower the energy loss due to desolvation by adding different alkyl substituents to the amine, amidine, or guanidine. The inhibition potency of all compounds was first tested at 1 and 0.1 μM. Promising compounds were then subjected to a more accurate AlphaScreen assay for IC_{50} determination. We first started with replacing the primary amine of **6** with different kinds of tertiary amines through reductive amination of key aldehyde intermediate **46** (Scheme 1B), which resulted in **7**−**11** (Table 1 and Supporting Information, Figure S2). IC_{50} measurement showed that compounds tended to be more potent as the ring size of the substitutional groups on the tertiary amine decreased. Among them, **11** that has a four-membered ring azetidine moiety exhibited the most potency with an IC_{50} value as 51 nM in inhibiting the interaction between His-ENL and biotin-

https://doi.org/10.1021/acs.jmedchem.1c00367
J. Med. Chem. XXXX, XXX, XXX−XXX

H3K9ac. These results suggest that the azetidine ring assists the binding to ENL. Further modifications were then introduced to **11** to afford **12**–**14** with different alkyl groups on the 2′ position of azetidine, which we wished to increase the electron density on the N atom and enhance the interaction between azetidine and Glu26. However, these compounds displayed lower potency than **11**. Given that Glu26 is located at a loop area with much conformational flexibility, we moved the azetidine moiety from the para to meta position affording **15** but did not result in any increase of potency. We also attempted to increase the rigidity of the molecule by adding a methyl group to the benzylic carbon affording **16**. However, it greatly reduced the inhibition potency. We also substituted the triazolopyridine moiety with similar heterocycles to afford **17**–**19**, but none of these compounds outcompeted **11** (Table 1, Scheme 1C and Supporting Information, Figure S2).

In addition to amine derivatives, we also designed a series of amidine derivatives based on compound **6** to afford **20**–**23**. These compounds were synthesized from corresponding nitrile intermediates, followed by acid-catalyzed ethanolysis and then ammonolysis (Scheme 2A). However, none of these compounds showed improved potency. Although an amidine or guanidine tend to form a stronger salt bridge with a carboxylate than an amine, it may have a higher desolvation energy than an amine, contributing to weak binding to ENL. For this reason, we focused the synthesis of additional amidine and guanidine derivatives **24**–**28** that have higher hydrophobicity than **20**–**23**. These compounds were synthesized by directly reacting **6** with corresponding N-heterocycle building blocks, except for compound **27**, which was made through 5-fluoro-2-aminopyridine due to the inadequate reactivity of 5-fluoro-2-chloropyridine in the reaction with **6** (Scheme 2B). Among them, **24** exhibited an IC_{50} value as 85 nM. **11** and **24** are the two most potent compounds in our compound series. We further evaluated their binding to ENL using the surface plasmon resonance (SPR) analysis. His-ENL was immobilized on dextran-coated Au chips through 1-ethyl-3-(3-dimethylaminopropyl)carbodiimide (EDCI)/*N*-hydroxy succinimide (NHS) coupling, followed by flow-through of a buffer containing different concentrations of **11** and **24**. The responses in sensorgrams were fitted to the Langmuir 1:1 binding kinetics model to obtain both association and dissociation rate constants, from which K_d values were then determined (Supporting Information, Figure S3A). Compared to the kinetics of typical small molecule–protein interactions, both association and dissociation of **11** and **24** toward ENL are relatively slow (association: 1800 and 1600 $M^{-1}\cdot s^{-1}$; dissociation: 8.3×10^{-5} and 7.0×10^{-5} s^{-1}, respectively). Their determined K_d values by SPR were 45 and 46 nM, respectively. As far as we know, **11** and **24** are the two most potent inhibitors for ENL that have so far been developed.

Small-Molecule Inhibitors Occupy the Same Binding Site of the ENL YEATS Domain as the Histone Acyl-lysine. To study the molecular basis of **7**, **11**, and **24** binding to ENL, we attempted to cocrystalize the ENL YEATS domain with these compounds, but it was not successful. We then modeled these compounds to the acetyllysine binding pocket of the ENL YEATS domain by docking analysis. **7** and **11** were docked in their protonated form, while **24** was docked in the neutral form, given that it is less likely to be much protonated under physiological pH. In the modeled structures (Figure 2A–D), all three compounds interact with ENL similar to **6** (Figure 1D). The amide forms two hydrogen bonds with S58

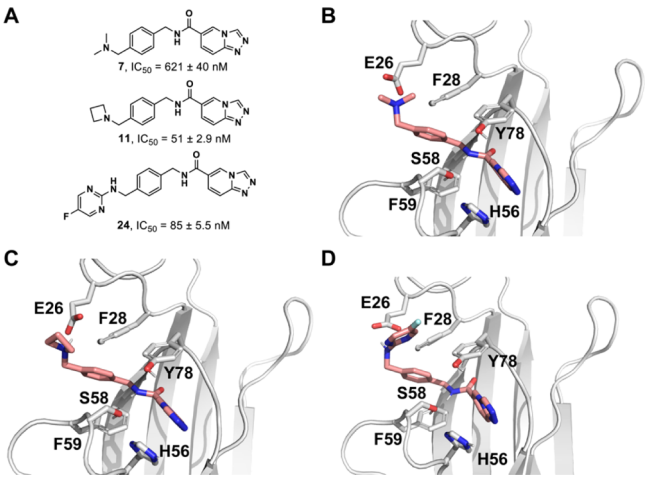

Figure 2. Compounds **7**, **11**, and **24** and their docking models bound to the ENL YEATS domain. (A) Chemical structures of compounds **7**, **11**, and **24** and their IC_{50} values in inhibiting the His-ENL–H3K9ac interaction in the AlphaScreen assay. (B–D) Molecular docking models of compounds **7** (B), **11** (C), and **24** (D) bound to the ENL YEATS domain. Modeling was based on the crystal structure of the ENL YEATS domain (PDB: 5J9S). Compounds are shown in stick representation, and the ENL YEATS domain is shown as a cartoon in gray. Compound-interacting residues of ENL are highlighted and shown in stick representation.

and Y78. The triazolopyridine ring was involved in π-stacking interactions with H56 in a parallel configuration and with Y78 in a T-shaped configuration. The phenyl group was also involved in π-stacking interactions with F28 and F59, both in a T-shaped configuration. Importantly, the amine of **7**, the azetidine of **11**, and the guanidine of **24** are all within 3 Å to E26, suggesting a common salt bridge or hydrogen bond interaction that stabilizes their interactions with ENL (Figure 2B–D).

To experimentally validate that **7** binds to the acyl-lysine binding pocket of ENL, we compared the binding of **7** and a H3K27cr peptide (histone H3 residues 22–31 with a crotonylation at K27) to ENL by nuclear magnetic resonance (NMR) spectroscopy.[33] We expressed ^{15}N-labeled His-ENL and recorded its ^{1}H, ^{15}N heteronuclear single quantum coherence (HSQC) spectra, while **7** or the H3K27cr peptide was titrated into the sample (Figure 3 and Supporting Information, Figure S3B). As expected, the H3K27cr peptide induced large chemical shift perturbations (CSPs) in the ENL YEATS domain, which were in the intermediate to fast exchange regime on the NMR timescale. Addition of **7** caused CSPs in the intermediate to slow exchange regime, indicating

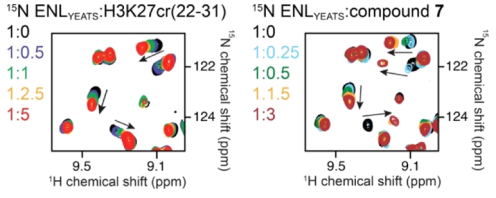

Figure 3. Compound **7** and the H3K27cr peptide occupy the same binding site of the ENL YEATS domain. Superimposed ^{1}H,^{15}N HSQC spectra of His-ENL collected as H3K27cr (H3 residues 22–31, left) or **7** (right) was added stepwise. Spectra are color-coded according to the protein/ligand molar ratios.

https://doi.org/10.1021/acs.jmedchem.1c00367
J. Med. Chem. XXXX, XXX, XXX–XXX

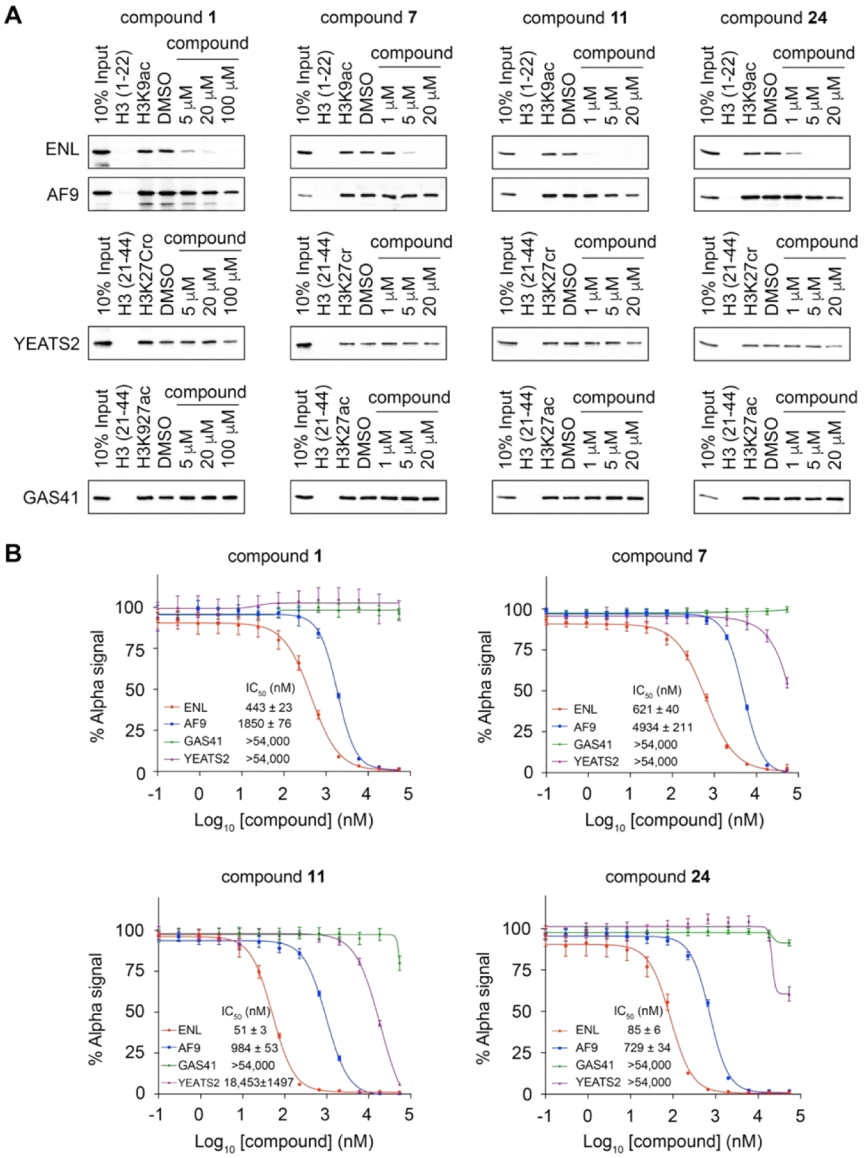

Figure 4. Compounds **7**, **11**, and **24** are highly specific to ENL over other YEATS domains. (A) Peptide pull-downs of ENL, AF9, YEATS2, and GAS41 with the indicated acylated histone peptides with or without **1**, **7**, **11**, and **24**. Unmodified histone peptides were used as negative controls to the acylated peptides and DMSO as a negative control to compound treatment. (B) AlphaScreen measurement of IC_{50} of **1**, **7**, **11**, and **24** in inhibition of YEATS domains binding to the corresponding acylated histone peptides as in (A). Data represent mean ± standard errors of the mean (SEM), $n = 4$.

that the ENL YEATS domain binds to **7** tighter than to the H3K27cr peptide. An overall similar pattern of CSPs observed in both experiments suggest that **7** and the H3K27cr peptide occupy the same binding site in the ENL YEATS domain.

Compounds 7, 11, and 24 Are Highly Selective toward the ENL YEATS Domain over All Other Human YEATS Domains. To determine whether the small-molecule inhibitors are selective toward ENL among the four human YEATS domains, we assessed **7**, **11**, and **24** in their inhibition of ENL, AF9, GAS41, and YEATS2 in peptide pull-down assays. We also included the original hit **1** in the assays for comparison. We used the H3K9ac peptide for AF9 and ENL, the H3K27ac peptide for GAS41, and the H3K27cr peptide for YEATS2 as these peptides are the preferred ligands of the corresponding YEATS domains.[7,11,14,16] We found 1 μM of **11** and **24** and 5 μM of **1** and **7** strongly inhibited the binding of ENL to H3K9ac, whereas at even a 20 μM concentration, none of these compounds showed notable inhibition to AF9, GAS41, or YEATS2 binding to their corresponding acylated histone peptides (Figure 4A). We further measured the IC_{50} values of **1**, **7**, **11**, and **24** in their inhibition of the binding of four human YEATS domains to their preferred histone peptide ligands using AlphaScreen assays. All four compounds displayed preferential inhibition of ENL over the other three YEATS domains. Compound **1** showed ~4-fold higher potency toward ENL than AF9, whereas no detectable inhibition was measured for the YEATS2 or GAS41 YEATS domain. Compounds **7**, **11**, and **24** exhibited even higher specificity to ENL. Particularly, the IC_{50} value of **11** to ENL was ~20-fold lower than that to AF9 (ENL IC_{50} 51 nM and AF9 IC_{50} 984 nM) (Figure 4B). As the previously reported small-molecule ENL inhibitors are not able to differentiate between ENL and AF9, our compounds provide promising

https://doi.org/10.1021/acs.jmedchem.1c00367
J. Med. Chem. XXXX, XXX, XXX−XXX

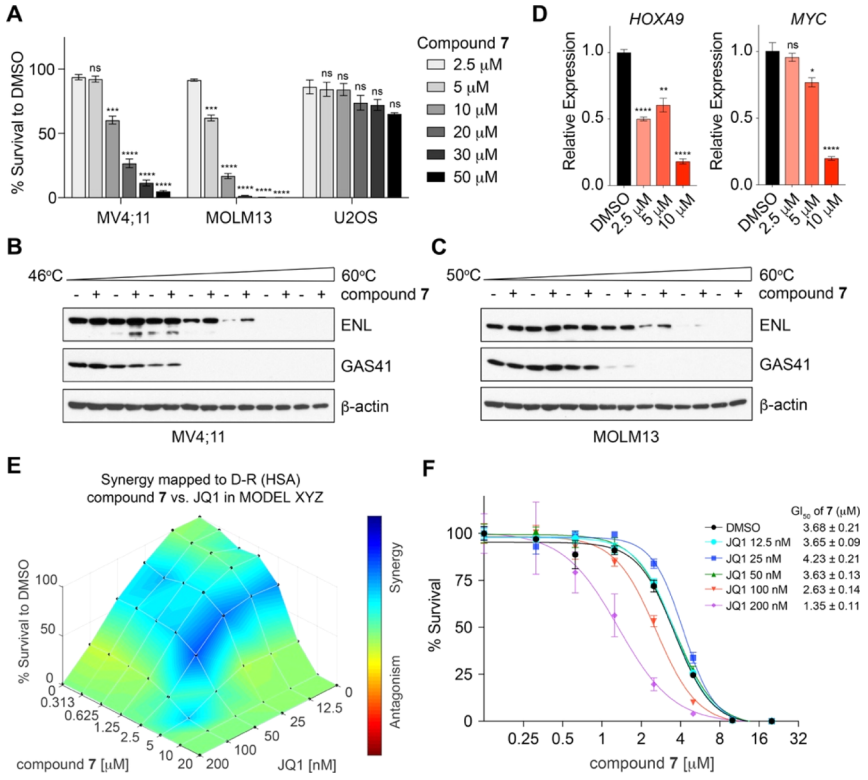

Figure 5. Compound 7 exhibits on-target effect of ENL inhibition in *MLL*-rearranged leukemia cell lines. (A) 7 inhibits leukemia cell growth. Cell growth inhibition of 7 at various concentrations in MV4-11, MOLM13, and U2OS cells. Survived cells were calculated as % relative to DMSO-treated cells. (B,C) CETSAs in MV4-11 (B) and MOLM13 (C) cells treated with 20 μM 7 at the indicated temperatures. β-Actin was used as a loading control. (D) qRT-PCR analysis of *HOXA9* and *MYC* gene expression in MOLM13 cells treated with 7 or the DMSO negative control. (E,F) 7 shows a synergistic effect with JQ1 in MOLM13 cells. (E) 3D synergy distribution of 7 and JQ1. MOLM13 cells were treated with indicated doses of 7 and JQ1 or DMSO for 6 days. Surviving cells were calculated as % relative to DMSO-treated cells. Synergistic interactions were analyzed using the Combenefit software. (F) GI_{50} of 7 when cotreated with indicated concentrations of JQ1. Data in (A,D) are shown as mean ± SEM, $n = 3$, two-tailed Student's *t*-test, ns, not significant, $^{*}P < 0.05$, $^{**}P < 0.005$, $^{***}P < 0.001$, $^{****}P < 0.0001$. Data in (E,F) represent mean ± SEM, $n = 3$.

scaffolds for further development of ENL-specific inhibitors for the study of ENL biology and for disease intervention.

Compound 7 Inhibits the Endogenous ENL Protein in *MLL*-Rearranged Cell Lines. To explore the small molecule ENL inhibitors we developed in biological applications, we first analyzed their cellular effects in MV4-11 and MOLM13 cells, two MLL-rearranged cell lines whose growth is dependent on ENL.[14,22] We screened 15 compounds with *in vitro* IC_{50} values lower than 2 μM, and we found 7 as the most potent compound in cell growth inhibition (Supporting Information, Figure S4A). The discrepancy between *in vitro* IC_{50} and cellular efficacy is not due to cell permeability as 7 was comparable to **11** in the standard Caco-2 permeability assay (Supporting Information, Figure S4B). Compound 7 exhibited ~40% inhibition of MOLM13 cell growth at 5 μM and 80% inhibition at 10 μM concentrations, while around double amounts of the compound were needed to achieve similar levels of inhibition in MV4-11 cells (Figure 5A). In contrast, U2OS cells, an ENL-independent cell line, showed little or no response to the treatment with 7, even at 50 μM.

Next, we asked whether the growth inhibition effect was caused by on-target inhibition of the endogenous ENL protein. In this regard, we carried out the cellular thermal shift assay (CETSA) to evaluate thermal stability of the ENL protein in MV4-11 and MOLM13 cells treated with 7. As the AF9 protein is undetectable in these cells with commercial antibodies, we evaluated thermal stability of the GAS41 protein for comparison. Compared to the DMSO-treated cells, we detected higher abundance of soluble ENL proteins in cells treated with 7, indicating that 7 bound and stabilized ENL proteins.[34] In contrast, the thermal stability of GAS41 proteins showed little or no difference between DMSO and 7 treatment (Figure 5B,C). Similarly, 7 stabilized ENL but not AF9 proteins in HeLa cells (Supporting Information, Figure S4C). The CETSA results suggest specific engagement of ENL with 7 in living cells.

We also evaluated the expression of two ENL target genes, *HOXA9* and *MYC*, in MOLM13 cells. Compound 7 effectively suppressed *HOXA9* gene expression at as low as 2.5 μM of drug concentration. At 10 μM, it suppressed ~80% of the expression of both *HOXA9* and *MYC* genes, comparable to the levels of gene suppression in *ENL* knock-down cells (Figure 5D and Supporting Information, S4D), suggesting potent and on-target effect of the ENL inhibitor.

Compound 7 Exhibits a Synergistic Effect with JQ1. Previously we found that CRISPR/Cas9-mediated ENL knockout sensitized leukemia cells to JQ1, an effective inhibitor of BET bromodomain proteins including BRD4.[4,14] An intriguing question was whether 7 has any synergy with JQ1 in killing leukemia cells. To answer this question, we carried out combinatory treatment of MV4-11 and MOLM13 cells with series of concentrations of 7 (0 to 20 μM) and JQ1 (0−200 nM). In both cell lines, we observed synergistic effect between ENL inhibition and JQ1 (Figure 5E and Supporting

https://doi.org/10.1021/acs.jmedchem.1c00367
J. Med. Chem. XXXX, XXX, XXX−XXX

Information, Figure S4E).[35] Particularly, at a concentration of 200 nM of JQ1, the GI_{50} of compound **7** in MOLM13 cells was reduced from 3.64 to 1.34 μM (Figure 5F). Together, these results demonstrate therapeutic potentials of the ENL inhibitors for future exploration in disease treatment.

DISCUSSION

The YEATS domain is a newly identified family of histone acylation readers. The four human YEATS domain-containing proteins, ENL, AF9, YEATS2, and GAS41, are subunits of protein complexes involved in chromatin and transcription regulation.[18,19] The evolutionally conserved histone-reading function of the YEATS domains is essential for the functionality of all the YEATS domain proteins in both yeasts and humans.[6−16] Dysregulation of the YEATS domain-containing proteins has been associated with various human diseases, including cancers. We and others showed that ENL and particularly, its YEATS domain is essential for disease maintenance and progression of acute leukemias.[14,22] Recently, we also found that the reader function of the ENL YEATS domain is indispensable for the aberrant gene activation and tumorigenesis caused by the gain-of-function ENL YEATS domain mutations identified in Wilms' tumor patients.[25] In addition, YEATS2 and GAS41 are frequently amplified in various types of human cancers.[36−38] All these studies suggest that the YEATS domains are promising drug targets, and therefore, targeting the YEATS domains may provide a novel therapeutic approach for a broad spectrum of human cancers.

Developing YEATS-domain inhibitors has been a research focus of the epigenetic reader field in recent years. The initial efforts were focused on targeting the YEATS domain of ENL because of great therapeutic potentials. Both small-molecule chemical compounds and peptide-mimic probes have recently been developed as acetyllysine competitive inhibitors of the ENL YEATS domain.[26−32] However, target selectivity has been a big challenge because the YEATS domains share high structural similarity, especially between ENL and its close homologue AF9. The few small-molecule ENL inhibitors reported so far have poor specificity that fail to distinguish ENL from AF9. The peptide-mimic chemical probes developed by the Li group showed slightly higher potency to the ENL YEATS domain than other YEATS domains, largely due to interactions outside of the acetyllysine binding pocket.[30] These results suggest that targeting both the acyl-lysine-binding pocket and additional proximal sites outside of the binding pocket might be a good approach to develop specific inhibitors. Indeed, based on this concept, the Li group has recently developed a conformationally preorganized cyclopeptide that showed a 38-fold higher binding affinity toward AF9 YEATS over ENL.[29]

Despite the success in developing peptide-mimic chemical probes specific to AF9, ENL-specific inhibitors were still lacking. Because ENL, but not AF9, is essential for *MLL*-rearranged acute leukemias and ENL mutant Wilms' tumors, it is in urgent need to develop ENL specific inhibitors for further drug development. In our study, through HTS, we identified compound **1**, which showed a 4-fold preference toward ENL over AF9 YEATS. After several rounds of structure-based inhibitor design and SAR studies, we were able to develop several compounds with much better selectivity. In particular, the IC_{50} value of compound **11** to ENL was ∼20-fold lower over AF9, ∼360-fold lower over YEATS2, and more than 1000-fold lower over GAS41, providing a good lead for future drug development.

The selectivity of our compounds to ENL over AF9 is intriguing, given that the AF9 YEATS domain has a 10-fold higher affinity than ENL YEATS in acyl-lysine binding. The YEATS domains of AF9 and ENL share a high degree of structural similarity.[11,14] It is not clear what interactions contribute to the ENL selectivity. By comparing the modeled structures of compounds **1**, **7**, **11**, and **24** docked to the acetyllysine binding pocket of the ENL and AF9 YEATS domains, we observed that the triazolopyridine pharmacophore of these compounds adopts conformations to form stronger $\pi-\pi$ interactions with the H56 residue in ENL than in the AF9 YEATS domain. When bound with the ENL YEATS domain, the distances between the triazole rings and the imidazole rings range from 3.4 to 3.6 Å and their dihedral angles range from 20 to 22°, whereas in the case of AF9 YEATS domain, the distances between them increase to 4.3−4.6 Å and their dihedral angles also increase to a range of 28−37°, both leading to weaker $\pi-\pi$ interactions compared to those in the ENL YEATS domain (Supporting Information, Figure S5). Additionally, the salt-bridge interaction in the case of **7** and **11** and the hydrogen bond for **24** with E26 in the ENL YEATS domain may also contribute to selectivity. Further structural study of YEATS domains in complex with these compounds will provide insights to guide future development of more potent and selective ENL YEATS-domain inhibitors.

In leukemia cells, our synthesized compound **7** exhibited clear on-target cellular effects in reducing ENL target gene expression and suppressing leukemia cell growth. In addition, consistent with previous results of genetic ENL ablation, **7** exhibited a synergistic effect with the BET bromodomain inhibitor JQ1 in killing leukemia cells. The cellular effects of our compounds are superior to all reported ENL inhibitors. Overall, our study provides valuable selective ENL small-molecule inhibitors that can serve as potential leads for further medicinal chemistry-based optimization to advance both basic and translational research of ENL. It also provides a molecular platform for the development of more complicated, multifunctional probes for applications such as visualization or targeted degradation in cells.

CONCLUSIONS

In this study, we carried out HTS of a small-molecule library of >66,000 compounds against the ENL YEATS domain and identified a series of hit molecules that share a [1,2,4]triazolo-[4,3-*a*]pyridine-6-amide pharmacophore and a common *N*,*C*-diarylamide scaffold. By introducing a potential salt-bridge interaction with E26 in ENL, we were able to generate compounds with IC_{50} and K_d values less than 100 nM. Importantly, our compounds outcompeted the previously reported ENL inhibitors by showing high selectivity toward ENL over AF9, the close paralogue of ENL. Furthermore, compound **7** exhibited on-target effect in inhibiting ENL target gene expression and leukemia cell growth. Our ENL-specific YEATS-domain inhibitors provide the basis for development of potent ENL-specific chemical probes in the future.

EXPERIMENTAL SECTION

Materials. The biotinylated histone peptides used in the AlphaScreen assay, H3 (aa 1−22, ARTKQTARKSTGGKAPRKQ-LAT), H3K9ac (aa 1−22, ARTKQTARK(ac)STGGKAPR-KQLAT), H3 (aa 21−44, ATKAARKSAPATGGVKKPHRYRPG), H3K27ac

https://doi.org/10.1021/acs.jmedchem.1c00367
J. Med. Chem. XXXX, XXX, XXX−XXX

(aa 21−44, ATKAARK(ac)SAPSTGGVKKPHRYRPG), H3K27cr (aa 21−44, ATKAARK(cro)SAPS-TGGVKKPHRYRPG), and the biotin-14× His peptide used in counter assay were purchased from CPC Scientific. Anti-ENL (14893S) antibody was from Cell Signaling, anti-GAS41 (sc-393708) and anti-glutathione-S-transferase (GST) (sc-459) antibodies were from Santa Cruz, and anti-AF9 (HPA001824) and anti-β-actin (A1978) antibody were from Sigma. Human cell lines MV4-11, MOLM13, U2OS, and HeLa cells were purchased from ATCC.

Protein Expression and Purification. The complementary DNA (cDNA) encoding sequences of four human YEATS domains: ENL (aa 1−145), AF9 (aa 1−145), full-length GAS41, and YEATS2 (aa 201−332) were cloned in pGEX-6P-1 and pET19b expression vectors, respectively. The His-tagged YEATS proteins were expressed in *Escherichia coli* Rosetta-2 (DE3) pLysS cells in the presence of 0.2 mM isopropyl-β-D-1-thiogalactopyranoside (IPTG) for 18 h at 16 °C. The His-tagged YEATS proteins were purified using Ni−nitrilotriacetic acid (NTA) resins following the manufacturer's instructions. The eluted protein was dialyzed in a buffer containing 50 mM *N*-(2-hydroxyethyl)piperazine-*N*′-ethanesulfonic acid (HEPES, pH 7.4), 100 mM NaCl, and 20% glycerol to remove imidazole. Proteins were adjusted to 0.5 mg/mL, aliquoted, and stored at −80 °C. Each batch of purified protein was tested in AlphaScreen assay conditions discussed as follows. The GST-tagged proteins used in peptide pull-down assays were expressed in the same way and purified using glutathione sepharose resins (GE Healthcare).

AlphaScreen Assay Setup. The AlphaScreen assay was carried out in 384-well plates. Manual assay setup was performed in a 30 μL reaction in α-reaction buffer (50 mM HEPES pH 7.4, 100 mM NaCl, 0.1% bovine serum albumin, and 0.05% CHAPS) with final concentrations of 100 nM His-ENL YEATS, 30 nM biotin-H3K9ac, and 10 μg/mL of AlphaScreen-donor and -acceptor beads. During the automation step, we were able to reduce the assay volume to 20 μL per well while maintaining the quality and robustness of the assay, with optimal final concentrations of His-ENL YEATS (100 nM), biotin-H3K9ac (10 nM), DMSO (0.1%), and AlphaScreen-beads (2.5 μg/mL). The protein, peptide, and compounds were mixed and incubated for 1 h at room temperature before adding the α beads. AlphaScreen-signals were detected by an EnVision microplate reader equipped with an Alpha-laser (PerkinElmer).

HTS Using AlphaScreen. High-throughput screening was performed at the Texas Screening Alliance for Cancer Therapeutics (TxSACT) facility. A total of 66,625 compounds screened were from Maybridge HitFinder Set (14,080), Chembridge Diversity Set (12,900), Chembridge Kinase Set (11,250), Chembridge Fragment Library (4000), ChemDiv Fragment Collection (14,143), Legacy Collection (2092), MicroSource Spectrum Collection (2000), LOPAC Collection (1275), Selleck Kinase and Bioactive Collection (2260), NCI Diversity (1595), NCI Mechanistic collection (820), and NCI natural products (210). In the primary HTS, fragments were screened at 50 μM and nonfragment compounds were screened at 10 μM. After the single-shot screen and hits triage, 990 hits were picked for confirmation assay and counter assay with biotin-14× His peptide.

IC_{50} Determination with the AlphaScreen Assay. The AlphaScreen assay conditions are essentially the same as the one used in high-throughput screening. The protein concentrations of AF9, Gas41, and YEATS2 are 30, 100, and 100 nM, respectively, and the peptide concentrations are 30 nM. All assays have been validated using protein and peptide competitors. For IC_{50} determination, compounds were subjected to eight threefold serial dilutions for a total of nine concentrations ranging from 50 μM to 8 nM for dose−response-curve AlphaScreen assays. IC_{50} values were determined from the plot using nonlinear regression of variable slope (four parameters) and curve fitting performed using GraphPad Prism.

Modeling of Inhibitors Bound with ENL and AF9 YEATS Domains. Molecular docking of target compounds was carried out using AutoDock 4.[39] The initial conformations of target compounds were first generated and MM2 minimized by PerkinElmer Chem3D software. Structures of the ENL and AF9 YEATS domains were obtained from PDB 5J9S and 4TMP, respectively, with H3K27ac and H3K9ac deleted from the complexes. Structures of the YEATS domains were then preprocessed in MGLTools 1.5.6 to remove water molecules and add polar hydrogens. The grid box was set to be centered at coordinates (x = 27.352, y = −42.139, z = 3.0) for ENL and at coordinates (x = 52.734, y = 10.522, z = −11.134) for AF9, with a size of 40 × 40 × 40 npts, which is big enough to contain the binding channel and surrounding amino acid residues. The Glu26 residue of the ENL YEATS domain was set to be flexible. The target compounds were then docked in the grid box. The conformations with lowest binding energies were converted to PDB files for visualization.

Compound Synthesis. All reagents and solvents for synthesis were purchased from commercial sources and used without purification. All glassware were flame-dried prior to use. Thin-layer chromatography (TLC) was carried out on aluminum plates coated with 60 F254 silica gel. TLC plates were visualized under UV light (254 or 365 nm) or stained with 5% phosphomolybdic acid. Normal-phase column chromatography was carried out using a Yamazen Smart Flash AKROS system. Analytical reverse-phase high-pressure liquid chromatography (RP-HPLC) was carried out on a Shimadzu LC20 HPLC system with an analytical C18 column. Semipreparative HPLC was carried out on the same system with a semipreparative C18 column. The mobile phases were H_2O with 0.1% formic acid (A) and acetonitrile with 0.1% formic acid (B) if not mentioned otherwise. NMR spectra were recorded on a Bruker AVANCE Neo 400 MHz or Varian INOVA 300 MHz spectrometer in specified deuterated solvents. High-resolution electrospray ionization mass spectrometry (HRMS-ESI) was carried out on a Thermo Scientific Q Exactive Focus system. The purities of compounds were confirmed by NMR and analytical HPLC-UV as ≥95%.

*tert-Butyl (4-(([1,2,4]Triazolo[4,3-a]pyridine-6-carboxamido)-methyl)benzyl)carbamate (**41**).* To a solution of **39** (1 mmol, 163 mg) and **40** (1 mmol, 236 mg) in dry dimethylformamide (DMF, 5 mL) were added DIPEA (2 mmol, 258 mg) and EDCI (1.2 mmol, 230 mg). The resulting solution was stirred at room temperature overnight. Then, the solution was diluted with EtOAc (50 mL) and washed with saturated $NaHCO_3$ solution (2 × 50 mL), 1 M HCl (2 × 50 mL), and saturated brine (50 mL). The organic layers were then dried with anhydrous Na_2SO_4 and then concentrated. The residue was purified by column chromatography (silica gel, 10% MeOH/DCM as the eluent) to yield **41** as a light-yellow solid (250 mg, 66%).

*(4-(([1,2,4]Triazolo[4,3-a]pyridine-6-carboxamido)methyl)-phenyl)methanamine Hydrochloride (**6**).* To a solution of **41** (0.5 mmol, 190 mg) in 5 mL of 1,4-dioxane was added 10 mL of 4 M HCl solution in 1,4-dioxane. The resulting solution was stirred at room temperature for 2 h. Then, the reaction mixture was concentrated to dryness *in vacuo* to yield **6** as a light-yellow solid (150 mg, 95%). ^{1}H NMR (400 MHz, deuterium oxide): δ 9.49 (s, 1H), 9.24 (s, 1H), 8.29 (dt, J = 9.7, 1.6 Hz, 1H), 8.10 (d, J = 9.6 Hz, 1H), 7.52−7.42 (m, 4H), 4.66 (s, 2H), 4.19 (s, 2H). ^{13}C NMR (101 MHz, D_2O): δ 165.4, 145.4, 138.5, 137.8, 134.1, 131.8, 129.2, 128.0, 127.4, 125.1, 112.1, 43.5, 42.7. ESI-HRMS (m/z): calcd for $C_{15}H_{16}N_5O$ $(M + H)^+$, 282.1349; found, 282.1344.

*4-(1,3-Dioxolan-2-yl)benzonitrile (**43**).* To a solution of **42** (38 mmol, 5.0 g) and ethylene glycol (76 mmol, 4.2 mL) in toluene (50 mL) was added pyridinium *p*-toluenesulfonate (4 mmol, 0.96 g). The resulting solution was heated to reflux with a Dean−Stark trap for 4 h. The resulting solution was then concentrated *in vacuo*, and the residue was then purified by column chromatography (silica gel, 10% EtOAc/hexanes as the eluent) to yield **43** as a white solid (5.25 g, 79%). ^{1}H NMR (300 MHz, chloroform-*d*): δ 7.67 (d, J = 8.3 Hz, 2H), 7.58 (d, J = 8.3 Hz, 2H), 5.84 (s, 1H), 4.17−3.99 (m, 4H).

*(4-(1,3-Dioxolan-2-yl)phenyl)methanamine (**44**).* $LiAlH_4$ (0.99 g, 26 mmol) was suspended in dry tetrahydrofuran (THF, 50 mL) and was cooled under 0 °C. A solution of **43** (4.5 g, 25.7 mmol) in dry THF (50 mL) was added dropwise to the $LiAlH_4$ suspension at the same temperature. After the addition, the reaction mixture was warmed up to room temperature and stirred for 4 h. Water (3 mL) was added dropwise, followed by 2 M aqueous NaOH solution (3 mL) and then, water (3 mL). The precipitate was filtered and washed

https://doi.org/10.1021/acs.jmedchem.1c00367
J. Med. Chem. XXXX, XXX, XXX−XXX

with THF. The combined filtrate was then dried with anhydrous Na_2SO_4 and evaporated *in vacuo*. The residue was then purified by column chromatography (silica gel, 100% EtOAc as the eluent) to yield **44** as a colorless oil to a white solid (3.0 g, 67%). ^{1}H NMR (300 MHz, chloroform-*d*): δ 7.44 (d, J = 8.1 Hz, 2H), 7.30 (d, J = 8.1 Hz, 2H), 5.78 (s, 1H), 4.15−3.95 (m, 4H), 3.85 (s, 2H).

*N-(4-(1,3-Dioxolan-2-yl)benzyl)-[1,2,4]triazolo[4,3-a]pyridine-6-carboxamide (**45**).* To a solution of **44** (2 mmol, 358 mg) and **39** (2 mmol, 326 mg) in DMF (10 mL) were added DIPEA (4 mmol, 516 mg) and EDCI (2.4 mmol, 460 mg). The resulting solution was then stirred at room temperature overnight. The reaction mixture was then diluted with EtOAc (50 mL) and then washed with saturated $NaHCO_3$ solution (2 × 50 mL), 1 M HCl (2 × 50 mL), and brine (50 mL). The organic layers were dried with anhydrous Na_2SO_4 and concentrated *in vacuo*. The residue was then purified by column chromatography (silica gel, 20% methanol/EtOAc as the eluent) to yield **45** as a white solid (520 mg, 80%). ^{1}H NMR (400 MHz, DMSO-d_6): δ 9.36 (d, J = 0.8 Hz, 1H), 9.25 (t, J = 5.9 Hz, 1H), 9.14 (t, J = 1.4 Hz, 1H), 7.90−7.76 (m, 2H), 7.44−7.33 (m, 4H), 5.70 (s, 1H), 4.52 (d, J = 5.8 Hz, 2H), 4.09−3.88 (m, 4H).

*N-(4-Formylbenzyl)-[1,2,4]triazolo[4,3-a]pyridine-6-carboxamide (**46**).* To a solution of **45** (520 mg, 1.6 mmol) in 1,4-dioxane (5 mL) was added 5 mL of 4 M HCl solution in 1,4-dioxane. The resulting solution was stirred for 2 h and concentrated *in vacuo*. The residue was suspended in H_2O and basified with saturated $NaHCO_3$ solution. The precipitation was filtered and dried to yield **46** as a yellowish solid (390 mg, 87%). ^{1}H NMR (400 MHz, DMSO-d_6): δ 9.99 (s, 1H), 9.42−9.31 (m, 2H), 9.16 (t, J = 1.4 Hz, 1H), 7.89 (d, J = 8.1 Hz, 2H), 7.87−7.78 (m, 2H), 7.57 (d, J = 7.9 Hz, 2H), 4.61 (d, J = 5.9 Hz, 2H).

*N-(4-((Dimethylamino)methyl)benzyl)-[1,2,4]triazolo[4,3-a]-pyridine-6-carboxamide (**7**).* To a solution of **46** (35 mg, 0.12 mmol) in THF (3 mL) was added a solution of dimethylamine in THF (1 M, 0.25 mL) and Ti(O^{i}Pr)$_4$ (0.36 mmol, 102 mg). The mixture was stirred at room temperature for 10 min. Then, $NaBH(OAc)_3$ (0.36 mmol, 76 mg) was added, and the mixture was refluxed under N_2. The reaction was monitored by TLC. Small additional portions of $NaBH(OAc)_3$ were added to drive the reaction to completion. Upon complete consumption of **46**, the reaction mixture was diluted with saturated $NaHCO_3$ solution (20 mL), and the precipitate was filtered. The filtrate was then extracted by EtOAc (2 × 20 mL). The combined organic layers were dried with anhydrous Na_2SO_4 and concentrated *in vacuo*. The residue was then purified by column chromatography (silica gel, 20% methanol/EtOAc as the eluent) to give **7** as a white solid (11 mg, 30%). ^{1}H NMR (400 MHz, methanol-d_4): δ 9.29 (d, J = 0.8 Hz, 1H), 9.09 (t, J = 1.4 Hz, 1H), 7.91−7.76 (m, 2H), 7.57−7.44 (m, 4H), 4.65 (s, 2H), 4.29 (s, 2H), 2.83 (s, 6H). ^{13}C NMR (101 MHz, DMSO): δ 164.1, 148.8, 141.0, 138.1, 131.6, 129.5, 128.1, 127.4, 127.0, 121.5, 114.9, 59.5, 42.9, 41.8. ESI-HRMS (m/z): calcd for $C_{17}H_{20}N_5O$ (M + H)$^+$, 310.1662; found, 310.1654.

*N-(4-(Piperidin-1-ylmethyl)benzyl)-[1,2,4]triazolo[4,3-a]pyridine-6-carboxamide (**8**).* To a solution of **46** (35 mg, 0.12 mmol) in THF (3 mL) were added piperidine (20 mg, 0.24 mmol) and Ti(O^{i}Pr)$_4$ (0.36 mmol, 102 mg). The mixture was stirred at room temperature for 10 min. Then, $NaBH(OAc)_3$ (0.36 mmol, 76 mg) was added, and the mixture was refluxed under N_2. The reaction was monitored by TLC. Small portions of $NaBH(OAc)_3$ were added to drive the reaction to completion. Upon complete consumption of **46**, the reaction mixture was diluted with saturated $NaHCO_3$ solution (20 mL) and the precipitate was filtered. The filtrate was then extracted by EtOAc (2 × 20 mL). The combined organic layers were dried with anhydrous Na_2SO_4 and concentrated *in vacuo*. The residue was then purified by column chromatography (silica gel, 20% methanol/EtOAc as the eluent) to give **8** as a white solid (12 mg, 28%). ^{1}H NMR (400 MHz, methanol-d_4): δ 9.26 (d, J = 0.8 Hz, 1H), 9.04 (t, J = 1.4 Hz, 1H), 7.87−7.76 (m, 2H), 7.38−7.29 (m, 4H), 4.60 (s, 2H), 3.50 (s, 2H), 2.37 (t, J = 5.1 Hz, 4H), 1.58 (p, J = 5.6 Hz, 4H), 1.45 (p, J = 5.6 Hz, 2H). ^{13}C NMR (101 MHz, MeOD): δ 164.8, 149.0, 137.5, 137.5, 135.9, 129.9, 127.4, 127.3, 126.4, 122.5, 114.2, 62.9, 53.8, 43.1, 25.0, 23.7. ESI-HRMS (m/z): calcd for $C_{20}H_{24}N_5O$ (M + H)$^+$, 350.1975; found, 350.1970.

*N-(4-(Morpholinomethyl)benzyl)-[1,2,4]triazolo[4,3-a]pyridine-6-carboxamide (**9**).* To a solution of **46** (35 mg, 0.12 mmol) in THF (3 mL) were added morpholine (21 mg, 0.24 mmol) and Ti(O^{i}Pr)$_4$ (0.36 mmol, 102 mg). The mixture was stirred at room temperature for 10 min. Then, $NaBH(OAc)_3$ (0.36 mmol, 76 mg) was added and the mixture was refluxed under N_2. The reaction was monitored by TLC. Small portions of additional $NaBH(OAc)_3$ were added to drive the reaction to completion. Upon complete consumption of **46**, the reaction mixture was diluted with saturated $NaHCO_3$ solution (20 mL) and the precipitate was filtered. The filtrate was then extracted by EtOAc (2 × 20 mL). The combined organic layers were dried with anhydrous Na_2SO_4 and concentrated *in vacuo*. The residue was then purified by column chromatography (silica gel, 20% methanol/EtOAc as the eluent) to give **9** as a white solid (15 mg, 43%). ^{1}H NMR (400 MHz, DMSO-d_6): δ 9.37 (s, 1H), 9.22 (t, J = 5.9 Hz, 1H), 9.14 (t, J = 1.4 Hz, 1H), 7.87−7.75 (m, 2H), 7.32−7.24 (m, 4H), 4.49 (d, J = 5.8 Hz, 2H), 3.55 (t, J = 4.7 Hz, 4H), 3.42 (s, 2H), 2.37−2.27 (m, 4H). ^{13}C NMR (101 MHz, DMSO): δ 163.5, 148.4, 137.8, 137.6, 136.5, 129.0, 127.3, 126.8, 126.4, 121.1, 114.4, 66.2, 62.1, 53.1, 42.5. ESI-HRMS (m/z): calcd for $C_{19}H_{22}N_5O_2$ (M + H)$^+$, 352.1768; found, 352.1764.

*N-(4-(Pyrrolidin-1-ylmethyl)benzyl)-[1,2,4]triazolo[4,3-a]-pyridine-6-carboxamide (**10**).* To a solution of **46** (35 mg, 0.12 mmol) in THF (3 mL) were added pyrrolidine (17 mg, 0.24 mmol) and Ti(O^{i}Pr)$_4$ (0.36 mmol, 102 mg). The mixture was stirred at room temperature for 10 min. Then, $NaBH(OAc)_3$ (0.36 mmol, 76 mg) was added and the mixture was refluxed under N_2. The reaction was monitored by TLC. Small portions of $NaBH(OAc)_3$ were added to drive the reaction to completion. Upon complete consumption of **46**, the reaction mixture was diluted with saturated $NaHCO_3$ solution (20 mL) and the precipitate was filtered. The filtrate was then extracted by EtOAc (2 × 20 mL). The combined organic layers were dried with anhydrous Na_2SO_4 and concentrated *in vacuo*. The residue was then purified by column chromatography (silica gel, 20% methanol/EtOAc as the eluent) to give **10** as a white solid (15 mg, 38%). ^{1}H NMR (300 MHz, methanol-d_4): δ 9.28 (s, 1H), 9.07 (d, J = 1.6 Hz, 1H), 7.86 (dd, J = 9.7, 1.7 Hz, 1H), 7.79 (d, J = 9.7 Hz, 1H), 7.41 (s, 4H), 4.61 (s, 2H), 3.94 (s, 2H), 3.02−2.76 (m, 4H), 1.97−1.88 (m, 4H). ^{13}C NMR (75 MHz, CD_3OD): δ 164.8, 149.0, 138.8, 137.5, 134.0, 129.7, 127.7, 127.4, 126.4, 122.4, 114.2, 58.8, 53.4, 43.0, 22.6. ESI-HRMS (m/z): calcd for $C_{19}H_{22}N_5O$ (M + H)$^+$, 336.1819 (M + H); found, 336.1810.

*N-(4-(Azetidin-1-ylmethyl)benzyl)-[1,2,4]triazolo[4,3-a]pyridine-6-carboxamide (**11**).* To a solution of **46** (35 mg, 0.12 mmol) in THF (3 mL) were added azetidine hydrochloride (22 mg, 0.24 mmol) and Ti(O^{i}Pr)$_4$ (0.36 mmol, 102 mg). The mixture was stirred at room temperature for 10 min. Then, $NaBH(OAc)_3$ (0.36 mmol, 76 mg) was added and the mixture was refluxed under N_2. The reaction was monitored by TLC. Small portions of additional $NaBH(OAc)_3$ were added to drive the reaction to completion. Upon complete consumption of **46**, the reaction mixture was diluted with saturated $NaHCO_3$ solution (20 mL) and the precipitate was filtered. The filtrate was then extracted by EtOAc (2 × 20 mL). The combined organic layers were dried with anhydrous Na_2SO_4 and concentrated *in vacuo*. The residue was then purified by column chromatography (silica gel, 20% methanol/EtOAc as the eluent) to give **11** as a white solid (15 mg, 40%). ^{1}H NMR (400 MHz, methanol-d_4): δ 9.29 (d, J = 0.8 Hz, 1H), 9.09 (t, J = 1.4 Hz, 1H), 7.91−7.76 (m, 2H), 7.52−7.42 (m, 4H), 4.63 (s, 2H), 4.30 (s, 2H), 4.06 (t, J = 8.1 Hz, 4H), 2.47 (p, J = 8.1 Hz, 2H). ^{13}C NMR (101 MHz, MeOD): δ 166.3, 150.4, 141.7, 138.9, 131.2, 130.9, 129.5, 128.8, 127.8, 123.7, 115.6, 59.2, 55.2, 44.3, 17.2. ESI-HRMS (m/z): calcd for $C_{18}H_{20}N_5O$ (M + H)$^+$, 322.1662; found, 322.1654.

*N-(4-((2-Methylazetidin-1-yl)methyl)benzyl)-[1,2,4]triazolo[4,3-a]pyridine-6-carboxamide (**12**).* To a solution of **46** (58 mg, 0.2 mmol) in DMF (1 mL) were added 2-methylazetidine hydrochloride (43 mg, 0.4 mmol) and Ti(O^{i}Pr)$_4$ (0.6 mmol, 170 mg). The mixture was stirred at room temperature for 10 min. Then, $NaBH(OAc)_3$ (0.6

https://doi.org/10.1021/acs.jmedchem.1c00367
J. Med. Chem. XXXX, XXX, XXX−XXX

mmol, 127 mg) was added, and the mixture was heated to 70−75 °C for 24 h under N_2. The reaction mixture was diluted with saturated $NaHCO_3$ solution (20 mL), and the precipitate was filtered. The filtrate was then extracted by EtOAc (2 × 30 mL). The combined organic layers were dried with anhydrous Na_2SO_4 and concentrated *in vacuo*. The residue was then purified by column chromatography (silica gel, 20% methanol/EtOAc as the eluent) to give **12** as a white solid (58 mg, 88%). ^{1}H NMR (400 MHz, methanol-d_4): δ 9.22 (d, J = 0.8 Hz, 1H), 9.02 (t, J = 1.4 Hz, 1H), 7.80 (dd, J = 9.6, 1.6 Hz, 1H), 7.71 (dt, J = 9.6, 1.0 Hz, 1H), 7.31−7.20 (m, 4H), 4.54 (s, 2H), 3.58 (d, J = 12.4 Hz, 1H), 3.46 (d, J = 12.4 Hz, 1H), 3.35−3.27 (m, 1H), 3.24−3.15 (m, 1H), 2.89 (dt, J = 9.8, 7.7 Hz, 1H), 2.04 (dtd, J = 10.2, 7.8, 2.3 Hz, 1H), 1.72 (tt, J = 10.0, 8.5 Hz, 1H), 0.97 (d, J = 6.2 Hz, 3H). ^{13}C NMR (101 MHz, CD_3OD): δ 167.0, 151.2, 139.8, 139.7, 138.3, 131.5, 129.7, 129.6, 128.6, 124.7, 116.4, 64.8, 63.7, 53.1, 45.3, 27.4, 22.1. ESI-HRMS (m/z): calcd for $C_{19}H_{22}N_5O$ $(M + H)^+$, 336.1819; found, 336.1814.

*N-(4-((2-Isopropylazetidin-1-yl)methyl)benzyl)-[1,2,4]triazolo-[4,3-a]pyridine-6-carboxamide (**13**).* To a solution of **46** (58 mg, 0.2 mmol) in DMF (1 mL) were added 2-isopropylazetidine hydrochloride (54 mg, 0.4 mmol) and $Ti(O^iPr)_4$ (0.6 mmol, 170 mg). The mixture was stirred at room temperature for 10 min. Then, $NaBH(OAc)_3$ (0.6 mmol, 127 mg) was added, and the mixture was heated to 70−75 °C for 24 h under N_2. The reaction mixture was diluted with saturated $NaHCO_3$ solution (20 mL), and the precipitate was filtered. The filtrate was then extracted by EtOAc (2 × 30 mL). The combined organic layers were dried with anhydrous Na_2SO_4 and concentrated *in vacuo*. The residue was then purified by column chromatography (silica gel, 20% methanol/EtOAc as the eluent) to give **13** as a white solid (61 mg, 84%). ^{1}H NMR (400 MHz, methanol-d_4): δ 9.29 (dt, J = 1.9, 0.9 Hz, 1H), 9.08 (ddt, J = 4.2, 2.8, 1.4 Hz, 1H), 7.91−7.77 (m, 2H), 7.46−7.33 (m, 4H), 4.62 (s, 2H), 4.18−4.03 (m, 1H), 3.90−3.65 (m, 1H), 3.43 (s, 1H), 3.39−3.34 (m, 1H), 3.22 (d, J = 8.8 Hz, 1H), 2.25 (d, J = 10.6 Hz, 1H), 2.07−1.95 (m, 1H), 1.85 (dd, J = 14.8, 8.4 Hz, 1H), 0.95 (dd, J = 6.7, 0.8 Hz, 3H), 0.85 (dd, J = 6.7, 2.8 Hz, 3H). ESI-HRMS (m/z): calcd for $C_{21}H_{25}N_5O$ $(M + H)^+$, 364.2132; found, 364.2128.

*N-(4-((2-(tert-Butyl)azetidin-1-yl)methyl)benzyl)-[1,2,4]triazolo-[4,3-a]pyridine-6-carboxamide (**14**).* To a solution of **46** (48 mg, 0.165 mmol) in DMF (1 mL) were added 2-*tert*-butyl azetidine hydrochloride (50 mg, 0.33 mmol) and $Ti(O^iPr)_4$ (0.495 mmol, 141 mg). The mixture was stirred at room temperature for 10 min. Then, $NaBH(OAc)_3$ (0.495 mmol, 105 mg) was added, and the mixture was heated to 70−75 °C for 24 h under N_2. The reaction mixture was diluted with saturated $NaHCO_3$ solution (20 mL), and the precipitate was filtered. The filtrate was then extracted by EtOAc (2 × 30 mL). The combined organic layers were dried with anhydrous Na_2SO_4 and concentrated *in vacuo*. The residue was then purified by column chromatography (silica gel, 20% methanol/EtOAc as the eluent) to give **14** as a white solid (50 mg, 80%). ^{1}H NMR (400 MHz, methanol-d_4): δ 9.30 (d, J = 0.8 Hz, 1H), 9.07 (t, J = 1.4 Hz, 1H), 7.92−7.79 (m, 2H), 7.40−7.29 (m, 4H), 4.61 (s, 2H), 3.95 (d, J = 12.9 Hz, 1H), 3.47−3.37 (m, 1H), 3.19−2.98 (m, 2H), 2.76 (d, J = 9.0 Hz, 1H), 2.01−1.85 (m, 2H), 0.93 (s, 9H). ESI-HRMS (m/z): calcd for $C_{22}H_{27}N_5O$ $(M + H)^+$, 378.2288; found, 378.2286.

*N-(3-(Azetidin-1-ylmethyl)benzyl)-[1,2,4]triazolo[4,3-a]pyridine-6-carboxamide (**15**).* To a solution of **47** (22 mg, 0.125 mmol) and **39** (27 mg, 0.14 mmol) in DMF (0.4 mL) were added 2-(1H-benzotriazole-1-yl)-1,1,3,3-tetramethyluronium hexafluorophosphate (HBTU) (52 mg, 0.14 mmol) and DIPEA (33 mg, 0.25 mmol). The resulting solution was then stirred at room temperature overnight. The reaction mixture then diluted with EtOAc (30 mL) and then washed with saturated $NaHCO_3$ solution (2 × 5 mL) and brine (5 mL). The organic layers were dried with anhydrous Na_2SO_4 and concentrated *in vacuo*. The residue was then purified by column chromatography (silica gel, 20% methanol/EtOAc as the eluent) to yield **15** as a white solid (25 mg, 62%). ^{1}H NMR (400 MHz, methanol-d_4): δ 9.30 (d, J = 0.9 Hz, 1H), 9.09 (t, J = 1.4 Hz, 1H), 7.94−7.79 (m, 2H), 7.38−7.30 (m, 3H), 7.24 (d, J = 1.0 Hz, 1H), 4.63 (s, 2H), 3.63 (s, 2H), 3.31 (t, J = 7.2 Hz, 4H), 2.21−2.07 (m, 2H). ESI-HRMS (m/z): calcd for $C_{18}H_{20}N_5O$ $(M + H)^+$, 322.1662; found, 322.1656.

*Methyl 4-(1-Aminoethyl)benzoate (**49**).* Methyl 4-acetylbenzoate (500 mg, 2.8 mmol), ammonium acetate (1.29 g, 16.8 mmol), and sodium cyanoborohydrate (263 mg, 4.2 mmol) were dissolved in 10 mL of methanol, and the solution was stirred at room temperature for 16 h. The reaction mixture was concentrated and acidified with 2 M HCl (5 mL) and then extracted with DCM. The aqueous layer was basified with solid $NaHCO_3$ and extracted with DCM (2 × 30 mL). The combined DCM layers were dried over Na_2SO_4 and concentrated. The residue was used without further purification.

*Methyl 4-(1-((tert-Butoxycarbonyl)amino)ethyl)benzoate (**50**).* Methyl 4-(1-aminoethyl)benzoate **49** (250 mg, 1.39 mmol) was dissolved in DCM (5 mL), and Boc anhydride (348 mg, 1.6 mmol), DIPEA (0.5 mL, 2.7 mmol), and 4-dimethylaminopyridine (DMAP) (17 mg, 0.139 mmol) were added and stirred for overnight. The reaction was washed with water and extracted with ethyl acetate (2 × 20 mL). The combined organic layers were dried over Na_2SO_4, concentrated, and purified by silica gel column chromatography (20% EtOAc/hexane) to yield **50** as a white solid (300 mg, 77%).

*tert-Butyl (1-(4-(Hydroxymethyl)phenyl)ethyl)carbamate (**51**).* Methyl 4-(1-((*tert*-butoxycarbonyl)amino)ethyl)benzoate **50** (0.3 g, 1.0 mmol) was dissolved in THF (3 mL), and the solution cooled to below −5 °C in an ice/salt bath. $LiAlH_4$ (2 M in THF, 1 mL) was added dropwise over 10 min. Upon completion of addition, the reaction was stirred at 0 °C for 75 min. Water (0.16 mL) was added dropwise, followed by 2 M aqueous NaOH solution (0.16 mL) and then, water (0.16 mL). The suspension was stirred for 15 min and then diluted with EtOAc (15 mL). The mixture was dried over Na_2SO_4 and filtered, and the resulting filtrate was concentrated *in vacuo* to afford the title compound, which was used without further purification (215 mg, 80%).

*tert-Butyl (1-(4-(Chloromethyl)phenyl)ethyl)carbamate (**52**).* To a stirred solution of **51** (200 mg, 0.8 mmol) in DCM (5 mL) were added methanesulfonyl chloride (108 mg, 0.95 mmol) and triethylamine (0.23 mL, 1.6 mmol). The solution was stirred for 16 h at room temperature and then washed with water and brine. After separation, the organic phase was dried over Na_2SO_4, filtered, and concentrated. The residue was purified by silica gel column chromatography (EtOAc/hexane 0 to 80%) to yield **52** as a white solid (100 mg, 46% yield).

*tert-Butyl (1-(4-(Azetidin-1-ylmethyl)phenyl)ethyl)carbamate (**53**).* To a stirred solution of **52** (100 mg, 0.37 mmol) in acetonitrile (5 mL) were added azetidine hydrochloride (41 mg, 0.44 mmol) and DIPEA (0.2 mL, 1.1 mmol). The solution was stirred at 80 °C for 16 h. The reaction mixture was diluted with water and extracted with DCM. The DCM layers were dried over Na_2SO_4 and concentrated to yield the crude product, which was used without further purification (100 mg).

*1-(4-(Azetidin-1-ylmethyl)phenyl)ethan-1-amine (**54**).* To a stirred solution of **53** (100 mg, 0.3 mmol), 4 M HCl in 1,4-dioxane (0.5 mL, 1.8 mmol) was added and stirred at room temperature for 1 h. The reaction mixture was concentrated to yield **54** as an off-white solid. ESI-HRMS (m/z): calcd for $C_{12}H_{19}N_2$ $(M + H)^+$, 191.1543; found, 191.1539.

*N-(1-(4-(Azetidin-1-ylmethyl)phenyl)ethyl)-[1,2,4]triazolo[4,3-a]-pyridine-6-carboxamide (**16**).* To a stirred solution of **39** (50 mg, 0.3 mmol) and **54** (58 mg, 0.3 mmol) in DMF (1 mL) were added HBTU (136 mg, 0.36 mmol) and DIPEA (0.1 mL, 0.6 mmol). The solution was stirred at room temperature for 16 h. The reaction mixture was diluted with water and extracted with DCM. The DCM layers were dried over Na_2SO_4 and concentrated to give the crude product, which was purified by flash chromatography to yield compound **16** as an off-white solid (30 mg, 34%). ^{1}H NMR (400 MHz, DMSO-d_6): δ 9.37 (s, 1H), 9.13 (s, 1H), 8.99 (d, J = 7.9 Hz, 1H), 7.90−7.72 (m, 2H), 7.32 (d, J = 7.5 Hz, 2H), 7.21 (d, J = 7.8 Hz, 2H), 5.14 (dd, J = 13.9, 7.1 Hz, 1H), 3.47 (s, 2H), 3.08 (t, J = 6.8 Hz, 4H), 1.94 (dd, J = 13.4, 6.9 Hz, 2H), 1.47 (d, J = 7.0 Hz, 3H). ESI-HRMS (m/z): calcd for $C_{19}H_{22}N_5O$ $(M + H)^+$, 336.1819; found, 336.1808.

https://doi.org/10.1021/acs.jmedchem.1c00367
J. Med. Chem. XXXX, XXX, XXX−XXX

*N-(4-(Azetidin-1-ylmethyl)benzyl)-[1,2,4]triazolo[4,3-a]pyridine-7-carboxamide (**17**).* To a solution of **55** (44 mg, 0.25 mmol) and **56** (45 mg, 0.275 mmol) in DMF (1 mL) were added HBTU (104 mg, 0.275 mmol) and DIPEA (65 mg, 0.5 mmol). The resulting solution was then stirred at room temperature overnight. The reaction mixture then diluted with EtOAc (30 mL) and then washed with saturated $NaHCO_3$ solution (2 × 5 mL) and brine (5 mL). The organic layers were dried with anhydrous Na_2SO_4 and concentrated *in vacuo*. The residue was then purified by column chromatography (silica gel, 20% methanol/EtOAc as the eluent) to yield **17** as a white solid (52 mg, 65%). ^{1}H NMR (400 MHz, methanol-d_4): δ 9.27 (s, 1H), 8.58 (d, J = 7.2 Hz, 1H), 8.26 (s, 1H), 7.44 (d, J = 7.3 Hz, 1H), 7.37 (d, J = 7.8 Hz, 2H), 7.29 (d, J = 7.1 Hz, 2H), 4.61 (s, 2H), 3.61 (s, 2H), 3.32−3.26 (m, 4H), 2.12 (p, J = 7.2 Hz, 2H). ESI-HRMS (m/z): calcd for $C_{18}H_{20}N_5O$ $(M + H)^+$, 322.1662; found, 322.1653.

*N-(4-(Azetidin-1-ylmethyl)benzyl)-[1,2,4]triazolo[1,5-a]pyridine-6-carboxamide (**18**).* To a solution of **55** (44 mg, 0.25 mmol) and **57** (45 mg, 0.275 mmol) in DMF (1 mL) were added HBTU (104 mg, 0.275 mmol) and DIPEA (65 mg, 0.5 mmol). The resulting solution was then stirred at room temperature overnight. The reaction mixture was then diluted with EtOAc (30 mL) and then washed with saturated $NaHCO_3$ solution (2 × 5 mL) and brine (5 mL). The organic layers were dried with anhydrous Na_2SO_4 and concentrated *in vacuo*. The residue was then purified by column chromatography (silica gel, 20% methanol/EtOAc as the eluent) to yield **18** as a white solid (49 mg, 61%). ^{1}H NMR (400 MHz, methanol-d_4): δ 9.34 (s, 1H), 8.52 (d, J = 1.4 Hz, 1H), 8.14 (dd, J = 9.3, 1.9 Hz, 1H), 7.86 (d, J = 9.3 Hz, 1H), 7.38 (d, J = 7.7 Hz, 2H), 7.30 (d, J = 7.3 Hz, 2H), 4.62 (s, 2H), 3.65 (s, 2H), 3.36 (d, J = 4.2 Hz, 4H), 2.14 (p, J = 7.2 Hz, 2H). ESI-HRMS (m/z): calcd for $C_{18}H_{20}N_5O$ $(M + H)^+$, 322.1662; found, 322.1655.

*N-(4-(Azetidin-1-ylmethyl)benzyl)-2-methylpyrazolo[1,5-a]pyrimidine-6-carboxamide (**19**).* To a solution of **55** (44 mg, 0.25 mmol) and **58** (49 mg, 0.275 mmol) in DMF (1 mL) were added HBTU (104 mg, 0.275 mmol) and DIPEA (65 mg, 0.5 mmol). The resulting solution was then stirred at room temperature overnight. The reaction mixture was then diluted with EtOAc (30 mL) and then washed with saturated $NaHCO_3$ solution (2 × 5 mL) and brine (5 mL). The organic layers were dried with anhydrous Na_2SO_4 and concentrated *in vacuo*. The residue was then purified by column chromatography (silica gel, 20% methanol/EtOAc as the eluent) to yield **19** as a white solid (49 mg, 59%). ^{1}H NMR (400 MHz, methanol-d_4): δ 9.29 (d, J = 2.2 Hz, 1H), 8.88 (d, J = 2.2 Hz, 1H), 7.38 (d, J = 7.9 Hz, 2H), 7.29 (d, J = 8.0 Hz, 2H), 6.59 (s, 1H), 4.61 (s, 2H), 3.62 (s, 2H), 3.29 (d, J = 7.2 Hz, 4H), 2.53 (s, 3H), 2.13 (p, J = 7.2 Hz, 2H). ESI-HRMS (m/z): calcd for $C_{19}H_{22}N_5O$ $(M + H)^+$, 336.1819; found, 336.1812.

*tert-Butyl (4-(Bromomethyl)benzyl)carbamate (**60**).* To a solution of **59** (238 mg, 1 mmol) in DCM (2 mL) was added triphenylphosphine (316 mg, 1.2 mmol). Then, carbon tetrabromide (400 mg, 1.2 mmol) was added in portions in an ice−water bath. The reaction was left in the ice−water bath for another 3 h. Then, the reaction mixture was filtered and concentrated *in vacuo*. The residue was purified by column chromatography (10:1 hexanes/EtOAc) to yield **60** as a white solid (252 mg, 83%).

*tert-Butyl (4-(Cyanomethyl)benzyl)carbamate (**61**).* To a solution of **60** (150 mg, 0.5 mmol) in 2 mL of DMF was added NaCN (50 mg, 1 mmol). The reaction mixture was then stirred at 60 °C for 4 h. The reaction mixture was cooled and diluted with water and extracted with DCM. Combined DCM layers were dried over Na_2SO_4 and then concentrated to yield **61** as a white solid, which was used without further purification (96 mg, 78%).

*N-(4-(Cyanomethyl)benzyl)-[1,2,4]triazolo[4,3-a]pyridine-6-carboxamide (**63**).* To a solution of **61** (96 mg, 0.39 mmol) in 1 mL of 1,4-dioxane was added 4 M HCl solution in dioxane (4 mL). The reaction mixture was stirred at room temperature for 1 h and then concentrated to dryness *in vacuo*. The residue was dissolved in 2 mL of DMF, to which were added **39** (64 mg, 0.39 mmol), DIPEA (155 mg, 1.2 mmol), and HBTU (175 mg, 0.46 mmol). The reaction mixture was stirred at room temperature overnight, then diluted with DCM (20 mL), and washed with saturated $NaHCO_3$ solution (2 × 20 mL), 1 M HCl (2 × 20 mL), and brine. The combined DCM layer was dried over Na_2SO_4 and concentrated *in vacuo*. The residue was purified by flash chromatography (0−10% MeOH/DCM) to yield **63** as a pale-yellow solid (58 mg, 52%). ^{1}H NMR (300 MHz, DMSO-d_6): δ 9.37 (s, 1H), 9.29 (t, J = 5.7 Hz, 1H), 9.15 (t, J = 1.2 Hz, 1H), 7.90−7.66 (m, 2H), 7.43−7.23 (m, 4H), 4.50 (d, J = 5.8 Hz, 2H), 4.01 (s, 2H).

*N-(4-(2-Amino-2-iminoethyl)benzyl)-[1,2,4]triazolo[4,3-a]pyridine-6-carboxamide (**20**).* To 1.5 mL of absolute EtOH was dropwise added 1 mL of acetylchloride under N_2 at 0 °C. The solution was stirred at 0 °C for 5 min before a solution of **63** (20 mg, 0.069 mmol) in absolute EtOH (0.5 mL) was added. The reaction mixture was stirred at room temperature for 36 h. The reaction mixture was then evaporated to dryness under high vacuum. To the residue was added a 7 M NH_3 solution in methanol (1 mL). The reaction mixture was then stirred overnight and concentrated *in vacuo*. The residue was dissolved in 1 M HCl solution, washed with EtOAc to remove residual **63**, and then evaporated to dryness to yield **20** as its hydrochloride salt (17 mg, 71%). ^{1}H NMR (300 MHz, D_2O): δ 9.47 (s, 1H), 9.22 (s, 1H), 8.24 (dt, J = 9.6, 1.8 Hz, 1H), 8.08 (d, J = 9.6 Hz, 1H), 7.46 (d, J = 8.0 Hz, 2H), 7.38 (d, J = 8.0 Hz, 1H), 4.65 (s, 2H), 3.89 (s, 2H). ESI-HRMS (m/z): calcd for $C_{16}H_{17}N_6O$ $(M + H)^+$, 309.1458; found, 309.1451.

*tert-Butyl (3-(Hydroxymethyl)-4-methylbenzyl)carbamate (**65**).* 2-Methyl-5-cyanobenzoic acid **64** (5 mmol, 0.81 g) was dissolved in anhydrous THF (15 mL). A solution of $LiAlH_4$ in THF (1.0 M, 20 mL) was added dropwise to the solution under N_2 at 0 °C. After completion of addition, the reaction mixture was heated to reflux overnight. The solution was then cooled to room temperature and then to 0 °C. Water (5 mL) was added dropwise, followed by 2 M NaOH solution (5 mL). After stirring for another 10 min, the mixture was filtered over Celite. To the filtrate was added Boc_2O (5 mmol, 1.09 g), and the solution was stirred at room temperature for 4 h. The solution was then concentrated *in vacuo* to yield crude **65** as a yellow oil (0.75 g, 60%). ^{1}H NMR (300 MHz, chloroform-d): δ 7.28 (s, 1H), 7.16−7.09 (m, 2H), 4.84 (br s, 1H), 4.68 (d, J = 5.2 Hz, 2H), 4.27 (d, J = 5.9 Hz, 2H), 2.32 (s, 3H), 1.66 (s, 1H), 1.45 (s, 9H).

*tert-Butyl (3-(Bromomethyl)-4-methylbenzyl)carbamate (**66**).* To a solution of **65** (1.2 mmol, 300 mg) in DCM (10 mL) was added triphenylphosphine (1.44 mmol, 380 mg). Then, carbon tetrabromide (1.44 mmol, 480 mg) was added in portions at 0 °C. The reaction was stirred at 0 °C for 3 h. Then, the reaction mixture was filtered and concentrated *in vacuo*. The residue was purified by column chromatography (hexanes/EtOAc = 10:1) to yield **66** as a white solid (284 mg, 76%). ^{1}H NMR (300 MHz, chloroform-d): δ 7.23 (s, 1H), 7.19−7.13 (m, 2H), 4.81 (br s, 1H), 4.59 (s, 2H), 4.27 (d, J = 5.9 Hz, 2H), 2.40 (s, 3H), 1.46 (s, 9H).

*tert-Butyl (3-(Cyanomethyl)-4-methylbenzyl)carbamate (**67**).* To a solution of **66** (156 mg, 0.5 mmol) in 5 mL of DMF was added NaCN (50 mg, 1 mmol). The reaction mixture was then stirred at 60 °C for 4 h. The reaction mixture was cooled and diluted with water and extracted with DCM. The combined DCM layers were dried over Na_2SO_4 and then concentrated to yield **67** as a white solid, which was used without further purification (78 mg, 60%).

*N-(3-(Cyanomethyl)-4-methylbenzyl)-[1,2,4]triazolo[4,3-a]pyridine-6-carboxamide (**69**).* To a solution of **67** (78 mg, 0.3 mmol) in 1 mL of 1,4-dioxane was added 4 M HCl solution in dioxane (4 mL). The reaction mixture was stirred at room temperature for 1 h and then concentrated to dryness *in vacuo*. The residue was dissolved in 2 mL of DMF, to which was added **39** (49 mg, 0.3 mmol), DIPEA (116 mg, 0.9 mmol), and HBTU (137 mg, 0.36 mmol). The reaction mixture was stirred at room temperature overnight, then diluted with DCM (20 mL), and washed with saturated $NaHCO_3$ solution (2 × 20 mL), 1 M HCl (2 × 20 mL) and brine. The combined DCM layer was dried over Na_2SO_4 and concentrated *in vacuo*. The residue was purified by flash chromatography (0−10% MeOH/DCM) to yield **69** as a white solid (46 mg, 50%). ^{1}H NMR (300 MHz, DMSO-d_6): δ 9.37 (t, J = 0.7 Hz, 1H), 9.24 (t, J = 5.9 Hz, 1H), 9.14 (s, 1H), 7.88−7.76 (m,

https://doi.org/10.1021/acs.jmedchem.1c00367
J. Med. Chem. XXXX, XXX, XXX−XXX

2H), 7.32 (s, 1H), 7.25−7.18 (m, 2H), 4.47 (d, J = 5.9 Hz, 2H), 3.98 (s, 2H), 2.27 (s, 3H).

*N-(3-(2-Amino-2-iminoethyl)-4-methylbenzyl)-[1,2,4]triazolo-[4,3-a]pyridine-6-carboxamide (**21**).* To 1.5 mL of absolute EtOH was dropwise added 1 mL of acetylchloride under N_2 at 0 °C. The solution was stirred at 0 °C for 5 min before a solution of **69** (20 mg, 0.066 mmol) in absolute EtOH (0.5 mL) was added. The reaction mixture was stirred at room temperature for 36 h. The reaction mixture was then evaporated to dryness under high vacuum. To the residue was added a 7 M NH_3 solution in methanol (1 mL). The reaction mixture was then stirred overnight and concentrated *in vacuo*. The residue was dissolved in 1 M HCl solution and washed with EtOAc to remove residual **69**, then evaporated to dryness to yield **21** as its hydrochloride salt (14 mg, 60%). ^{1}H NMR (300 MHz, D_2O): δ 9.46 (s, 1H), 9.22 (s, 1H), 8.33 (d, J = 9.3 Hz, 1H), 8.08 (d, J = 9.2 Hz, 1H), 7.31−7.13 (m, 3H), 4.50 (s, 2H), 3.83 (s, 2H), 2.14 (s, 3H). ESI-HRMS (m/z): calcd for $C_{17}H_{19}N_6O$ $(M + H)^+$, 323.1615; found, 323.1611.

*tert-Butyl (3-Fluoro-4-(hydroxymethyl)benzyl)carbamate (**71**).* 2-Fluoro-4-cyanobenzoic acid **70** (5 mmol, 0.83 g) was dissolved in anhydrous THF (15 mL). A solution of $LiAlH_4$ in THF (1.0 M, 20 mL) was added dropwise to the above solution under N_2 at 0 °C. After completion of addition, the reaction mixture was heated to reflux overnight. The solution was then cooled to room temperature and then to 0 °C. Water (5 mL) was added dropwise, followed by 2 M NaOH solution (5 mL). After stirring for another 10 min, the mixture was filtered over Celite. To the filtrate was added Boc_2O (5 mmol, 1.09 g) and the solution was stirred at room temperature for 4 h. The solution was then concentrated *in vacuo* to yield crude **71** as a yellow oil (0.71 g, 55%).

*tert-Butyl (4-(Bromomethyl)-3-fluorobenzyl)carbamate (**72**).* To a solution of **71** (1.2 mmol, 306 mg) in DCM (10 mL) was added triphenylphosphine (1.44 mmol, 380 mg). Then, carbon tetrabromide (1.44 mmol, 480 mg) was added in portions at 0 °C. The reaction was stirred at 0 °C for 3 h. Then, the reaction mixture was filtered and concentrated *in vacuo*. The residue was purified by column chromatography (hexanes/EtOAc = 10:1) to yield **72** as a white solid (250 mg, 66%). ^{1}H NMR (300 MHz, chloroform-d): δ 7.34 (t, J = 7.8 Hz, 1H), 7.13−6.95 (m, 2H), 4.88 (br s, 1H), 4.50 (s, 2H), 4.30 (d, J = 6.2 Hz, 2H), 1.46 (s, 9H).

*tert-Butyl (4-(Cyanomethyl)-3-fluorobenzyl)carbamate (**73**).* To a solution of **72** (159 mg, 0.5 mmol) in 5 mL of DMF was added NaCN (50 mg, 1 mmol). The reaction mixture was then stirred under 60 °C for 4 h. The reaction mixture was cooled and diluted with water and extracted with DCM. The combined DCM layers were dried over Na_2SO_4 and then concentrated to yield **73** as a white solid, which was used without further purification (85 mg, 64%).

*N-(4-(Cyanomethyl)-3-fluorobenzyl)-[1,2,4]triazolo[4,3-a]-pyridine-6-carboxamide (**75**).* To a solution of **73** (79 mg, 0.3 mmol) in 1 mL of 1,4-dioxane was added 4 M HCl solution in dioxane (4 mL). The reaction mixture was stirred at room temperature for 1 h and then concentrated to dryness *in vacuo*. The residue was dissolved in 2 mL of DMF, to which were added **39** (49 mg, 0.3 mmol), DIPEA (116 mg, 0.9 mmol), and HBTU (137 mg, 0.36 mmol). The reaction mixture was stirred at room temperature overnight, then diluted with DCM (20 mL), and washed with saturated $NaHCO_3$ solution (2 × 20 mL), 1 M HCl (2 × 20 mL), and brine. The combined DCM layer was dried over Na_2SO_4 and concentrated *in vacuo*. The residue was purified by flash chromatography (0−10% MeOH/DCM) to yield **75** as a white solid (51 mg, 55%). ^{1}H NMR (300 MHz, methanol-d_4): δ 9.29 (s, 1H), 9.09 (s, 1H), 7.83 (t, J = 8.7 Hz, 2H), 7.46 (t, J = 7.8 Hz, 1H), 7.34−7.16 (m, 2H), 4.63 (s, 2H), 3.92 (s, 2H).

*N-(4-(2-Amino-2-iminoethyl)-3-fluorobenzyl)-[1,2,4]triazolo[4,3-a]pyridine-6-carboxamide (**22**).* To 1.5 mL of absolute EtOH was dropwise added 1 mL of acetylchloride under N_2 at 0 °C. The solution was stirred at 0 °C for 5 min before a solution of **75** (20 mg, 0.065 mmol) in absolute EtOH (0.5 mL) was added. The reaction mixture was stirred at room temperature for 36 h. The reaction mixture was then evaporated to dryness under high vacuum. To the residue was added a 7 M NH_3 solution in methanol (1 mL). The reaction mixture was then stirred overnight and concentrated *in vacuo*. The residue was dissolved in 1 M HCl solution and washed with EtOAc to remove residual **75** and then evaporated to dryness to yield **22** as its hydrochloride salt (10 mg, 47%). ^{1}H NMR (300 MHz, D_2O): δ 9.46 (s, 1H), 9.22 (s, 1H), 8.22 (dd, J = 9.6, 1.5 Hz, 1H), 8.06 (d, J = 9.6 Hz, 1H), 7.41 (t, J = 8.0 Hz, 1H), 7.33−7.14 (m, 2H), 4.63 (s, 2H), 3.93 (s, 2H). ESI-HRMS (m/z): calcd for $C_{16}H_{16}FN_6O$ $(M + H)^+$, 327.1364; found, 327.1352.

*tert-Butyl (4-Fluoro-3-(hydroxymethyl)benzyl)carbamate (**77**).* 2-Fluoro-5-cyanobenzoic acid **76** (5 mmol, 0.83 g) was dissolved in anhydrous THF (15 mL). A solution of $LiAlH_4$ in THF (1.0 M, 20 mL) was added dropwise to the solution under N_2 at 0 °C. After completion of addition, the reaction mixture was heated to reflux overnight. The solution was then cooled to room temperature and then to 0 °C. Water (5 mL) was added dropwise, followed by addition of 2 M NaOH solution (5 mL). After stirring for another 10 min, the mixture was filtered over Celite. To the filtrate was added Boc_2O (5 mmol, 1.09 g), and the solution was stirred at room temperature for 4 h. The solution was then concentrated *in vacuo* to yield crude **77** as a yellow oil (0.81 g, 59%).

*tert-Butyl (3-(Bromomethyl)-4-fluorobenzyl)carbamate (**78**).* To a solution of **77** (1.2 mmol, 306 mg) in DCM (10 mL) was added triphenylphosphine (1.44 mmol, 380 mg). Then, carbon tetrabromide (1.44 mmol, 480 mg) was added in portions at 0 °C. The reaction was stirred at 0 °C for 3 h. Then, the reaction mixture was filtered and concentrated *in vacuo*. The residue was purified by column chromatography (hexanes/EtOAc = 10:1) to yield **78** as a white solid (234 mg, 62%). ^{1}H NMR (300 MHz, chloroform-d): δ 7.34−7.27 (m, 1H), 7.25−7.18 (m, 1H), 7.05−6.96 (m, 1H), 4.87 (br s, 1H), 4.49 (s, 2H), 4.29 (d, J = 6.2 Hz, 2H), 1.46 (s, 9H).

*tert-Butyl (3-(Cyanomethyl)-4-fluorobenzyl)carbamate (**79**).* To a solution of **78** (159 mg, 0.5 mmol) in 5 mL of DMF was added NaCN (50 mg, 1 mmol). The reaction mixture was then stirred under 60 °C for 4 h. The reaction mixture was cooled and diluted with water and extracted with DCM. The combined DCM layers were dried over Na_2SO_4 and then concentrated to yield **79** as a white solid, which was used without further purification (79 mg, 60%).

*N-(3-(Cyanomethyl)-4-fluorobenzyl)-[1,2,4]triazolo[4,3-a]-pyridine-6-carboxamide (**81**).* To a solution of **79** (79 mg, 0.3 mmol) in 1 mL of 1,4-dioxane was added 4 M HCl solution in dioxane (4 mL). The reaction mixture was stirred at room temperature for 1 h and then concentrated to dryness *in vacuo*. The residue was dissolved in 2 mL of DMF, to which were added **39** (49 mg, 0.3 mmol), DIPEA (116 mg, 0.9 mmol), and HBTU (137 mg, 0.36 mmol). The reaction mixture was stirred at room temperature overnight, then diluted with DCM (20 mL), and washed with saturated $NaHCO_3$ solution (2 × 20 mL), 1 M HCl (2 × 20 mL), and brine. The combined DCM layer was dried over Na_2SO_4 and concentrated *in vacuo*. The residue was purified by flash chromatography (0−10% MeOH/DCM) to yield **81** as a white solid (57 mg, 62%). ^{1}H NMR (300 MHz, DMSO-d_6): δ 9.37 (s, 1H), 9.29 (t, J = 5.6 Hz, 1H), 9.14 (s, 1H), 7.85 (d, J = 9.6 Hz, 1H), 7.78 (dd, J = 9.7, 1.5 Hz, 1H), 7.48−7.20 (m, 3H), 4.50 (d, J = 6.1 Hz, 2H), 4.05 (s, 2H).

*N-(4-(2-Amino-2-iminoethyl)-3-fluorobenzyl)-[1,2,4]triazolo[4,3-a]pyridine-6-carboxamide (**23**).* To 1.5 mL of absolute EtOH was dropwise added 1 mL of acetylchloride under N_2 at 0 °C. The solution was stirred at 0 °C for 5 min before a solution of **81** (20 mg, 0.065 mmol) in absolution EtOH (0.5 mL) was added. The reaction mixture was stirred at room temperature for 36 h. The reaction mixture was then evaporated to dryness under high vacuum. To the residue was added a 7 M NH_3 solution in methanol (1 mL). The reaction mixture was then stirred overnight and concentrated *in vacuo*. The residue was dissolved in 1 M HCl solution, washed with EtOAc to remove residual **81**, and then evaporated to dryness to yield **23** as its hydrochloride salt (13 mg, 60%). ^{1}H NMR (300 MHz, D_2O): δ 9.51 (s, 1H), 9.27 (s, 1H), 8.35 (dd, J = 9.6, 1.6 Hz, 1H), 8.13 (d, J = 9.6 Hz, 1H), 7.50−7.34 (m, 2H), 7.27−7.10 (m, 1H), 4.62 (s, 2H),

https://doi.org/10.1021/acs.jmedchem.1c00367
J. Med. Chem. XXXX, XXX, XXX−XXX

3.91 (s, 2H). ESI-HRMS (m/z): calcd for $C_{16}H_{16}FN_6O$ $(M + H)^+$, 327.1364; found, 327.1359.

*N-(4-(((5-Fluoropyrimidin-2-yl)amino)methyl)benzyl)-[1,2,4]-triazolo[4,3-a]pyridine-6-carboxamide (**24**).* To a stirred solution of 2-chloro-5-fluoropyrimidine (24 mg, 0.18 mmol) and amine **6** (48 mg. 0.15 mmol) in ethanol (1 mL) was added DIPEA (0.1 mL, 0.57 mmol), and the reaction mixture was heated to 75 °C for 36 h. The reaction was concentrated and purified by flash chromatography (silica gel, 5% methanol/EtOAc as the eluent) to yield **24** as a light-yellow solid (22 mg, 39%). ^{1}H NMR (400 MHz, DMSO-d_6): δ 9.36 (s, 1H), 9.21 (t, J = 5.9 Hz, 1H), 9.12 (t, J = 1.4 Hz, 1H), 8.32 (d, J = 1.0 Hz, 2H), 7.86−7.73 (m, 3H), 7.26 (s, 4H), 4.46 (d, J = 5.9 Hz, 2H), 4.43 (d, J = 6.4 Hz, 2H). ^{13}C NMR (101 MHz, DMSO): δ 163.9, 159.9, 153.3, 150.9, 148.8, 146.1, 145.8, 139.4, 138.0, 137.8, 127.8, 127.5, 127.2, 126.9, 121.6, 114.9, 44.7, 43.0. ESI-HRMS (m/z): calcd for $C_{19}H_{17}FN_7O$ $(M + H)^+$, 378.1473; found, 378.1465.

*N-(4-(((5-Isopropylpyrimidin-2-yl)amino)methyl)benzyl)-[1,2,4]-triazolo[4,3-a]pyridine-6-carboxamide (**25**).* To a stirred solution of amine **6** (50 mg, 0.17 mmol) and 2-chloro-5-isopropylpyrimidine (15 mg, 0.17 mmol) in ethanol (2 mL) was added DIPEA (68 mg, 0.53 mmol) and heated to 80 °C for 48 h. The reaction mixture was concentrated and purified by flash chromatography (0−10% methanol/DCM) to yield **25** as an off-white solid (10 mg, 18%). ^{1}H NMR (400 MHz, DMSO-d_6): δ 9.35 (d, J = 0.8 Hz, 1H), 9.21 (t, J = 5.8 Hz, 1H), 9.13 (t, J = 1.4 Hz, 1H), 8.16 (s, 2H), 7.86−7.73 (m, 2H), 7.49 (t, J = 6.4 Hz, 1H), 7.26 (s, 4H), 4.49−4.40 (m, 4H), 2.71 (hept, J = 6.9 Hz, 1H), 1.15 (d, J = 6.9 Hz, 7H). ^{13}C NMR (101 MHz, DMSO-d_6): δ 163.9, 161.7, 156.5, 148.8, 139.9, 138.0, 137.7, 129.2, 127.7, 127.5, 127.2, 127.0, 121.6, 114.9, 44.3, 43.0, 28.7, 24.0. ESI-HRMS (m/z): calcd for $C_{22}H_{23}N_7ONa$ $(M + Na)^+$, 424.1856; found, 424.1849.

*N-(4-(((4,5-Dihydro-1H-imidazol-2-yl)amino)methyl)benzyl)-[1,2,4]triazolo[4,3-a]pyridine-6-carboxamide (**26**).* To a stirred solution of amine **6** (95 mg, 0.3 mmol) and **82** (70 mg, 0.6 mmol) in DMF (2 mL) was added triethylamine (91 mg, 0.9 mmol) and heated to 100 °C for 16 h. The reaction mixture was concentrated under reduced pressure. Water was added to the crude product, and the solid was filtered and concentrated under reduced pressure to provide the crude compound **26** (20 mg, 19%). The crude compound was purified by RP-HPLC (HPLC gradient: 0−70 min: 95% A to 50% A). ^{1}H NMR (300 MHz, DMSO-d_6): δ 9.38 (s, 1H), 9.28 (s, 1H), 9.14 (s, 1H), 8.67 (s, 1H), 7.82 (q, J = 9.7 Hz, 2H), 7.46−7.18 (m, 4H), 4.49 (d, J = 5.9 Hz, 2H), 4.35 (d, J = 5.9 Hz, 2H), 3.60 (s, 4H). ESI-HRMS (m/z): calcd for $C_{18}H_{20}N_7O$ $(M + H)^+$, 350.1724; found, 350.1724.

*tert-Butyl (4-(((5-Fluoropyridin-2-yl)amino)methyl)benzyl)-carbamate (**84**).* To a stirred solution of **83** (1 mmol, 300 mg) in 5 mL of DMF were added **60** (1 mmol, 112 mg) and K_2CO_3 (1 mmol, 138 mg). The reaction mixture was stirred at room temperature overnight. The reaction mixture was diluted with water (25 mL) and then extracted with DCM (2 × 20 mL). The organic layer was dried over anhydrous Na_2SO_4 and concentrated. The residue was then purified by flash chromatography to yield **84** as a white solid (100 mg, 30%). ^{1}H NMR (400 MHz, $CDCl_3$): δ 7.96 (d, J = 3.0 Hz, 1H), 7.31 (d, J = 7.9 Hz, 2H), 7.25 (d, J = 8.2 Hz, 2H), 7.19 (ddd, J = 9.0, 7.9, 3.0 Hz, 1H), 6.32 (dd, J = 9.1, 3.4 Hz, 1H), 4.84 (s, 2H), 4.46 (d, J = 5.6 Hz, 2H), 4.30 (d, J = 6.0 Hz, 2H), 1.46 (s, 9H).

*N-(4-(Aminomethyl)benzyl)-5-fluoropyridin-2-amine Dihydrochloride (**85**).* To a stirred solution of **84** (0.3 mmol, 100 mg) in 1,4-dioxane (1 mL) was added a 4 M HCl solution in dioxane (4 mL). The solution was stirred at room temperature for 1 h. The reaction mixture was then concentrated *in vacuo* to yield **85** as a white solid (85 mg, 95%), which was used without further purification.

*N-(4-(((5-Fluoropyridin-2-yl)amino)methyl)benzyl)-[1,2,4]-triazolo[4,3-a]pyridine-6-carboxamide (**27**).* To a stirred solution of **85** (54 mg, 0.18 mmol) and **39** (32 mg, 0.20 mmol) in DMF (2 mL) were added DIPEA (0.15 mL, 0.8 mmol) and HBTU (80 mg, 0.22 mmol). The solution was then stirred at room temperature overnight. The reaction mixture was then diluted with water (20 mL) and extracted with EtOAc (2 × 20 mL). The organic layer was dried over anhydrous Na_2SO_4 and concentrated. The residue was then purified by flash chromatography to provide **27** as a pale-yellow solid (38 mg, 56%). ^{1}H NMR (400 MHz, DMSO-d_6): δ 9.36 (d, J = 0.8 Hz, 1H), 9.21 (t, J = 5.9 Hz, 1H), 9.13 (t, J = 1.4 Hz, 1H), 7.90 (d, J = 3.1 Hz, 1H), 7.87−7.73 (m, 2H), 7.33 (td, J = 8.8, 3.1 Hz, 1H), 7.28 (s, 4H), 7.04 (t, J = 6.0 Hz, 1H), 6.51 (dd, J = 9.1, 3.6 Hz, 1H), 4.47 (d, J = 5.9 Hz, 2H), 4.40 (d, J = 6.0 Hz, 2H). ^{13}C NMR (101 MHz, DMSO): δ 163.5, 155.7, 153.7, 151.3, 148.4, 139.2, 137.6, 137.4, 133.5, 133.3, 127.3, 127.2, 126.7, 126.5, 125.1, 124.9, 121.1, 114.4, 108.8, 108.7, 44.4, 42.6. ESI-HRMS (m/z): calcd for $C_{20}H_{17}FN_6O$ $(M + H)^+$, 377.1521; found, 377.1520.

*N-(4-(((3,6-Difluoropyridin-2-yl)amino)methyl)benzyl)-[1,2,4]-triazolo[4,3-a]pyridine-6-carboxamide (**28**).* To a stirred solution of 2,3,6-trifluoropyridine (32 mg, 0.24 mmol) and amine **6** (63 mg, 0.2 mmol) in *N*-methyl-2-pyrrolidone (0.5 mL) was added DIPEA (0.1 mL, 0.57 mmol), and the reaction mixture was heated to 90 °C overnight. The reaction mixture was cooled, then diluted with EtOAc (25 mL), and then washed with brine (2 × 5 mL). The organic layers were dried with anhydrous Na_2SO_4 and concentrated *in vacuo*. The residue was then purified by column chromatography (silica gel, 5% methanol/EtOAc as the eluent) to yield **28** as a light-yellow solid (30 mg, 38%). ^{1}H NMR (400 MHz, methanol-d_4): δ 9.27 (d, J = 1.0 Hz, 1H), 9.04 (q, J = 1.4 Hz, 1H), 7.90−7.76 (m, 2H), 7.41−7.25 (m, 5H), 6.02 (dtd, J = 8.2, 3.1, 2.6, 1.3 Hz, 1H), 4.59 (d, J = 1.1 Hz, 2H), 4.57 (s, 2H). ESI-HRMS (m/z): calcd for $C_{20}H_{17}F_2N_6O$ $(M + H)^+$, 395.1426; found, 395.1426.

SPR Assay. All SPR experiments were performed on a Biosensing BI-4500 instrument with 1× PBS with 0.1% DMSO as the running buffer and a flow rate at 60 μL/min. His-ENL YEATS was immobilized through EDCI/NHS coupling on CM dextran-coated sensor chips (Biosensing). The sensor chip was activated by flowing 200 μL of 0.05 M NHS plus 0.2 M EDCI solution through the surface. Then, 200 μL of 6 μM His-ENL YEATS in 10 mM NaOAc/HOAc and 150 mM NaCl, pH 5.5, was injected and flowed through the activated surface. Then, 100 μL of 1 M ethanolamine pH 7.8 solution was injected to block the remaining activated ester on the surface. **11** and **24** were dissolved in the running buffer and subjected to a twofold serial dilution for a total of four concentrations ranging from 5.6 to 0.7 μM (for **24**, 5.4 to 0.675 μM). For each cycle, 350 μL of the compound solution was injected and flowed through the surface, followed by a 600 s delay for dissociation. Prior to the first cycle, 350 μL of the running buffer was injected for baseline calibration. A control flow channel was set up in parallel without His-ENL YEATS immobilization to subtract nonspecific binding signals. The data analysis was performed on the kinetic analysis software provided by Biosensing Instrument Inc. and fitted into the Langmuir 1:1 binding model.

NMR Experiments for the ENL YEATS Domain. For NMR experiments, the YEATS domain of ENL (aa 1−148) was expressed as a C-terminal, uncleavable 6× His fusion protein (plasmid was a generous gift from Oleg Fedorov). The ^{15}N-labeled protein was expressed in *E. coli* Rosetta-2 (DE3) pLysS cells grown in NH_4Cl (Sigma-Aldrich) minimal media. After induction with IPTG (final concentration 0.5 mM) (Gold Biotechnology) for 18 h at 16 °C, the cells were harvested *via* centrifugation and lysed by sonication. The uniformly ^{15}N-labeled YEATS domain was incubated with Ni−NTA resins (Thermo Fisher Scientific), washed and eluted with imidazole. The protein was further purified by size exclusion chromatography, concentrated (Millipore) and stored at −80 °C.

The NMR experiments were performed at 298 K on a Varian INOVA 600 MHz spectrometer. The ^{1}H,^{15}N HSQC spectra of a 0.2 mM uniformly ^{15}N-labeled YEATS domain (25−50 mM Tris-HCl pH 7.5 buffer, supplemented with 150 mM NaCl, 0.2 mM tris(2-carboxyethyl)phosphine and 10% D_2O) were collected in the presence of an increasing amount of the H3K27cr (aa 22−31) peptide (synthesized by Synpeptide) or compound **7**. NMR data were processed and analyzed with NMRPipe and NMRDraw, as previously described.[33]

Competitive Peptide Pull-Down Assay. Compounds at indicated concentrations were mixed with 2 μg of GST-fused

https://doi.org/10.1021/acs.jmedchem.1c00367
J. Med. Chem. XXXX, XXX, XXX−XXX

YEATS proteins in 300 μL of the binding buffer (50 mM Tris-HCl pH 7.5, 250 mM NaCl, 0.1% NP-40, 1 mM phenylmethylsulfonyl fluoride) and rotated at 4 °C for 1 h. Then, 0.5 μg of biotinylated histone peptides with different modifications were added and incubated for 4 h. Streptavidin magnetic beads (Amersham) were added to the mixture, and the mixture was incubated for 1 h with rotation. The beads were then washed 3 times and analyzed using sodium dodecyl sulfate-polyacrylamide gel electrophoresis (SDS-PAGE) and western blotting.

IC_{50} Determination in the Inhibition of YEATS Domains. To assess the specificity of **7**, **11**, and **24**, their IC_{50} values in inhibition of the four human YEATS domain proteins binding to targeted histone peptides were determined in AlphaScreen assays. The compounds were subjected to 12 threefold serial dilutions for a total of 13 concentrations ranging from 54 μM to 0.1 nM for the dose response curve. IC_{50} values were determined from the plot using nonlinear regression of variable slopes (four parameters) and curve fitting performed by the GraphPad Prism software.

Cell Growth Inhibition Assay. Human leukemia MV4-11 and MOLM13 cells were maintained in RPMI-1640 (Cellgro) supplemented with 10% fetal bovine serum (Sigma). Human U2OS cells were maintained in Dulbecco's modified Eagle medium (DMEM, Cellgro) supplemented with 10% fetal bovine serum. A total of 5000 cells were seeded in a 96-well plate in 100 μL of the medium, treated with DMSO or compounds at indicated concentrations for 3 days. Cell viability was measured using the CellTiter-Glo luminescent cell viability assay kit (Promega) according to the manufacturer's instructions. Surviviving cells were calculated as % relative to DMSO-treated cells.

RNA Extraction and qRT-PCR. Total RNA was extracted using the RNeasy plus kit (Qiagen) and reverse-transcribed using an iScript cDNA synthesis kit (Bio-Rad). Quantitative real-time PCR (qRT-PCR) analyses were performed as described previously using PowerUp SYBR Green PCR Master Mix and the Bio-Rad CFX96 real-time PCR detection system. Gene expressions were calculated following normalization to glyceraldehyde 3-phosphate dehydrogenase (GAPDH) levels using the comparative C_t (cycle threshold) method.

Cellular Thermal Shift Assay.[34] MOLM13, MV4-11, and HeLa cells were incubated with 20 μM of compound **7** for 5 h. The cells were then collected and washed with PBS 3 times. The cell pellets were resuspended in PBS-containing protease inhibitors and aliquoted into PCR microtubes (approximately 3 million cells in 54 μL). Cells were heated at indicated temperatures for 3 min in a thermal cycler (Bio-Rad) and then incubated at room temperature for 2 min. A total of 6 μL of 10× cell lysis buffer (8% NP-40, 50% glycerol, and 10 mM dithiothreitol) was added to each sample before subjecting to three freeze−thaw cycles by liquid nitrogen and 37 °C water bath incubations to lyse the cells. The cell lysates were centrifuged at 13,000 rpm at 4 °C for 10 min, and the supernatants were analyzed using SDS-PAGE and western blotting.

Caco-2 Cell Permeability Assay. The cell permeability assay was performed at Charles River Labs to measure the rate of flux of a compound across polarized Caco-2 cell monolayers. Ranitidine, talinolol, and warfarin were used as controls. All compounds were tested at 10 μM with 2 h incubation in triplicate. P_{app} (apparent permeability) in apical to basolateral (A−B) direction was calculated and used to predict the *in vivo* absorption of a compound. $P_{app} > 1 \times 10^{-6}$ cm/s is considered as higher permeability.

Combinatorial Treatment of Compound 7 and JQ1. MOLM13 or MV4-11 cells were treated with DMSO, compound **7**, JQ1, or a combination of compounds **7** and JQ1 at indicated concentrations for 6 days. Cell viability was measured using the CellTiter-Glo luminescent cell viability assay kit (Promega). Surviviving cells were calculated as % relative to DMSO-treated cells. Synergistic interactions were analyzed and visualized using the Combenefit software.[35]

Quantification and Statistical Analysis. All AlphaScreen assays were performed in 4−6 replicates. Raw signal readings were normalized to no compound controls. GraphPad Prism 9 was used for regression analysis for IC_{50} determination.

■ ASSOCIATED CONTENT

Supporting Information

The Supporting Information is available free of charge at https://pubs.acs.org/doi/10.1021/acs.jmedchem.1c00367.

Overview of screen assay development, IC_{50} of top compounds, SPR and NMR data, cell growth inhibition, cell permeability assay, CETSA result of **7** in HeLa, qRT-PCR data, synergistic effect of **7** and JQ1 in MV4-11, molecular docking models of compounds bound to AF9 and ENL YEATS domains, HPLC traces for lead compounds, and table of the structure and IC_{50} of compounds from HTS with IC_{50} below 5 μM (PDF)

Molecular formula strings (CSV)

Docking models (ZIP)

■ AUTHOR INFORMATION

Corresponding Authors

Wenshe Ray Liu − *Texas A&M Drug Discovery Laboratory, Department of Chemistry, Department of Biochemistry and Biophysics, and Department of Molecular and Cellular Medicine, College of Medicine, Texas A&M University, College Station, Texas 77843, United States; Institute of Biosciences and Technology and Department of Translational Medical Sciences, College of Medicine, Texas A&M University, Houston, Texas 77030, United States;* orcid.org/0000-0002-7078-6534; Email: wliu@chem.tamu.edu

Hong Wen − *Department of Epigenetics, Van Andel Institute, Grand Rapids, Michigan 49503, United States;* orcid.org/0000-0001-8739-4572; Email: Hong.Wen@vai.org

Authors

Xinyu R. Ma − *Texas A&M Drug Discovery Laboratory, Department of Chemistry, Texas A&M University, College Station, Texas 77843, United States*

Longxia Xu − *Department of Epigenetics, Van Andel Institute, Grand Rapids, Michigan 49503, United States*

Shiqing Xu − *Texas A&M Drug Discovery Laboratory, Department of Chemistry, Texas A&M University, College Station, Texas 77843, United States*

Brianna J. Klein − *Department of Pharmacology, University of Colorado School of Medicine, Aurora, Colorado 80045, United States*

Hongkuan Wang − *Department of Epigenetics, Van Andel Institute, Grand Rapids, Michigan 49503, United States*

Sukant Das − *Texas A&M Drug Discovery Laboratory, Department of Chemistry, Texas A&M University, College Station, Texas 77843, United States*

Kuai Li − *Department of Epigenetics, Van Andel Institute, Grand Rapids, Michigan 49503, United States*

Kai S. Yang − *Texas A&M Drug Discovery Laboratory, Department of Chemistry, Texas A&M University, College Station, Texas 77843, United States;* orcid.org/0000-0002-1890-4169

Sana Sohail − *Department of Epigenetics, Van Andel Institute, Grand Rapids, Michigan 49503, United States*

Andrew Chapman − *Texas A&M Drug Discovery Laboratory, Department of Chemistry, Texas A&M University, College Station, Texas 77843, United States*

https://doi.org/10.1021/acs.jmedchem.1c00367
J. Med. Chem. XXXX, XXX, XXX−XXX

Tatiana G. Kutateladze − *Department of Pharmacology, University of Colorado School of Medicine, Aurora, Colorado 80045, United States;* orcid.org/0000-0001-7375-6990
Xiaobing Shi − *Department of Epigenetics, Van Andel Institute, Grand Rapids, Michigan 49503, United States*

Complete contact information is available at: https://pubs.acs.org/10.1021/acs.jmedchem.1c00367

Author Contributions

△X.R.M. and L.X. contributed equally. Conceptualization, X.S., W.R.L., and H.W.; methodology, T.G.K., W.R.L., and H.W.; investigation, X.R.M., L.X., S.X., B.J.K., H.W., S.D., K.L., K.S.Y., S.S., and A.C.; writing—original draft, X.R.M., L.X., B.J.K., W.R.L., and H.W.; writing—review & editing, S.X., T.G.K., and X.S.; funding acquisition, X.S., T.G.K., W.R.L., and H.W.; supervision, T.G.K., X.S., W.R.L., and H.W.

Notes

The authors declare no competing financial interest.

■ ACKNOWLEDGMENTS

This work was supported by funds from NIH grants (GM135671 and CA252707) to T.G.K., the Cancer Prevention and Research Institute of Texas (RP160237) to X.S., Welch Foundation (A-1715), the Texas A&M X Grant Program, and the Texas A&M College of Science Strategic Transformative Research Program to W.R.L., and NIH grant (CA255506) and the Thomas and Garretta Newhof/Prein & Newhorf Research Fund to H.W.

■ ABBREVIATIONS

AF9, ALL1-fused gene from chromosome 9 protein; BET, bromodomain and extraterminal domain; CETSA, cellular thermal shift assay; CSP, chemical shift perturbations; DOT1L, disruptor of telomeric silencing 1-like; ENL, eleven-nineteen-leukemia protein; GAS41, glioma-amplified sequence 41; GI_{50}, half growth inhibition concentration; HTS, high-throughput screening; MLL, mixed-lineage leukemia; PTM, post-translational modification; SEC, super elongation complex; SEM, standard errors of the mean; SPR, surface plasmon resonance; YEATS domain, Yaf9, ENL, AF9, Taf14, and Sas5 domain; YEATS2, YEATS domain-containing protein 2

■ REFERENCES

(1) Jenuwein, T.; Allis, C. D. Translating the histone code. *Science* **2001**, *293*, 1074−1080.
(2) Strahl, B. D.; Allis, C. D. The language of covalent histone modifications. *Nature* **2000**, *403*, 41−45.
(3) Dawson, M. A.; Prinjha, R. K.; Dittmann, A.; Giotopoulos, G.; Bantscheff, M.; Chan, W.-I.; Robson, S. C.; Chung, C.-w.; Hopf, C.; Savitski, M. M.; Huthmacher, C.; Gudgin, E.; Lugo, D.; Beinke, S.; Chapman, T. D.; Roberts, E. J.; Soden, P. E.; Auger, K. R.; Mirguet, O.; Doehner, K.; Delwel, R.; Burnett, A. K.; Jeffrey, P.; Drewes, G.; Lee, K.; Huntly, B. J. P.; Kouzarides, T. Inhibition of BET recruitment to chromatin as an effective treatment for MLL-fusion leukaemia. *Nature* **2011**, *478*, 529−533.
(4) Filippakopoulos, P.; Qi, J.; Picaud, S.; Shen, Y.; Smith, W. B.; Fedorov, O.; Morse, E. M.; Keates, T.; Hickman, T. T.; Felletar, I.; Philpott, M.; Munro, S.; McKeown, M. R.; Wang, Y.; Christie, A. L.; West, N.; Cameron, M. J.; Schwartz, B.; Heightman, T. D.; La Thangue, N.; French, C. A.; Wiest, O.; Kung, A. L.; Knapp, S.; Bradner, J. E. Selective inhibition of BET bromodomains. *Nature* **2010**, *468*, 1067−1073.
(5) Dhalluin, C.; Carlson, J. E.; Zeng, L.; He, C.; Aggarwal, A. K.; Zhou, M.-M.; Zhou, M.-M. Structure and ligand of a histone acetyltransferase bromodomain. *Nature* **1999**, *399*, 491−496.
(6) Andrews, F. H.; Shinsky, S. A.; Shanle, E. K.; Bridgers, J. B.; Gest, A.; Tsun, I. K.; Krajewski, K.; Shi, X.; Strahl, B. D.; Kutateladze, T. G. The Taf14 YEATS domain is a reader of histone crotonylation. *Nat. Chem. Biol.* **2016**, *12*, 396−398.
(7) Hsu, C.-C.; Shi, J.; Yuan, C.; Zhao, D.; Jiang, S.; Lyu, J.; Wang, X.; Li, H.; Wen, H.; Li, W.; Shi, X. Recognition of histone acetylation by the GAS41 YEATS domain promotes H2A.Z deposition in non-small cell lung cancer. *Genes Dev.* **2018**, *32*, 58−69.
(8) Hsu, C.-C.; Zhao, D.; Shi, J.; Peng, D.; Guan, H.; Li, Y.; Huang, Y.; Wen, H.; Li, W.; Li, H.; Shi, X. Gas41 links histone acetylation to H2A.Z deposition and maintenance of embryonic stem cell identity. *Cell Discovery* **2018**, *4*, 28.
(9) Klein, B. J.; Ahmad, S.; Vann, K. R.; Andrews, F. H.; Mayo, Z. A.; Bourriquen, G.; Bridgers, J. B.; Zhang, J.; Strahl, B. D.; Côté, J.; Kutateladze, T. G. Yaf9 subunit of the NuA4 and SWR1 complexes targets histone H3K27ac through its YEATS domain. *Nucleic Acids Res.* **2018**, *46*, 421−430.
(10) Li, Y.; Sabari, B. R.; Panchenko, T.; Wen, H.; Zhao, D.; Guan, H.; Wan, L.; Huang, H.; Tang, Z.; Zhao, Y.; Roeder, R. G.; Shi, X.; Allis, C. D.; Li, H. Molecular coupling of histone crotonylation and active transcription by AF9 YEATS domain. *Mol. Cell* **2016**, *62*, 181−193.
(11) Li, Y.; Wen, H.; Xi, Y.; Tanaka, K.; Wang, H.; Peng, D.; Ren, Y.; Jin, Q.; Dent, S. Y. R.; Li, W.; Li, H.; Shi, X. AF9 YEATS domain links histone acetylation to DOT1L-mediated H3K79 methylation. *Cell* **2014**, *159*, 558−571.
(12) Mi, W.; Guan, H.; Lyu, J.; Zhao, D.; Xi, Y.; Jiang, S.; Andrews, F. H.; Wang, X.; Gagea, M.; Wen, H.; Tora, L.; Dent, S. Y. R.; Kutateladze, T. G.; Li, W.; Li, H.; Shi, X. YEATS2 links histone acetylation to tumorigenesis of non-small cell lung cancer. *Nat. Commun.* **2017**, *8*, 1088.
(13) Shanle, E. K.; Andrews, F. H.; Meriesh, H.; McDaniel, S. L.; Dronamraju, R.; DiFiore, J. V.; Jha, D.; Wozniak, G. G.; Bridgers, J. B.; Kerschner, J. L.; Krajewski, K.; Martín, G. M.; Morrison, A. J.; Kutateladze, T. G.; Strahl, B. D. Association of Taf14 with acetylated histone H3 directs gene transcription and the DNA damage response. *Genes Dev.* **2015**, *29*, 1795−1800.
(14) Wan, L.; Wen, H.; Li, Y.; Lyu, J.; Xi, Y.; Hoshii, T.; Joseph, J. K.; Wang, X.; Loh, Y.-H. E.; Erb, M. A.; Souza, A. L.; Bradner, J. E.; Shen, L.; Li, W.; Li, H.; Allis, C. D.; Armstrong, S. A.; Shi, X. ENL links histone acetylation to oncogenic gene expression in acute myeloid leukaemia. *Nature* **2017**, *543*, 265−269.
(15) Zhang, Q.; Zeng, L.; Zhao, C.; Ju, Y.; Konuma, T.; Zhou, M.-M. Structural insights into histone crotonyl-lysine recognition by the AF9 YEATS domain. *Structure* **2016**, *24*, 1606−1612.
(16) Zhao, D.; Guan, H.; Zhao, S.; Mi, W.; Wen, H.; Li, Y.; Zhao, Y.; Allis, C. D.; Shi, X.; Li, H. YEATS2 is a selective histone crotonylation reader. *Cell Res.* **2016**, *26*, 629−632.
(17) Le Masson, I.; Yu, D. Y.; Jensen, K.; Chevalier, A.; Courbeyrette, R.; Boulard, Y.; Smith, M. M.; Mann, C. Yaf9, a novel NuA4 histone acetyltransferase subunit, is required for the cellular response to spindle stress in yeast. *Mol. Cell. Biol.* **2003**, *23*, 6086−6102.
(18) Schulze, J. M.; Wang, A. Y.; Kobor, M. S. YEATS domain proteins: a diverse family with many links to chromatin modification and transcription. *Biochem. Cell Biol.* **2009**, *87*, 65−75.
(19) Schulze, J. M.; Wang, A. Y.; Kobor, M. S. Reading chromatin Insights from yeast into YEATS domain structure and function. *Epigenetics* **2010**, *5*, 573−577.
(20) Biswas, D.; Milne, T. A.; Basrur, V.; Kim, J.; Elenitoba-Johnson, K. S. J.; Allis, C. D.; Roeder, R. G. Function of leukemogenic mixed lineage leukemia 1 (MLL) fusion proteins through distinct partner protein complexes. *Proc. Natl. Acad. Sci. U.S.A.* **2011**, *108*, 15751−15756.
(21) He, N.; Chan, C. K.; Sobhian, B.; Chou, S.; Xue, Y.; Liu, M.; Alber, T.; Benkirane, M.; Zhou, Q. Human Polymerase-Associated

Factor complex (PAFc) connects the Super Elongation Complex (SEC) to RNA polymerase II on chromatin. *Proc. Natl. Acad. Sci. U.S.A.* **2011**, *108*, E636−E645.
(22) Erb, M. A.; Scott, T. G.; Li, B. E.; Xie, H.; Paulk, J.; Seo, H.-S.; Souza, A.; Roberts, J. M.; Dastjerdi, S.; Buckley, D. L.; Sanjana, N. E.; Shalem, O.; Nabet, B.; Zeid, R.; Offei-Addo, N. K.; Dhe-Paganon, S.; Zhang, F.; Orkin, S. H.; Winter, G. E.; Bradner, J. E. Transcription control by the ENL YEATS domain in acute leukaemia. *Nature* **2017**, *543*, 270−274.
(23) Gadd, S.; Huff, V.; Walz, A. L.; Ooms, A. H. A. G.; Armstrong, A. E.; Gerhard, D. S.; Smith, M. A.; Auvil, J. M. G.; Meerzaman, D.; Chen, Q.-R.; Hsu, C. H.; Yan, C.; Nguyen, C.; Hu, Y.; Hermida, L. C.; Davidsen, T.; Gesuwan, P.; Ma, Y.; Zong, Z.; Mungall, A. J.; Moore, R. A.; Marra, M. A.; Dome, J. S.; Mullighan, C. G.; Ma, J.; Wheeler, D. A.; Hampton, O. A.; Ross, N.; Gastier-Foster, J. M.; Arold, S. T.; Perlman, E. J. A Children's Oncology Group and TARGET initiative exploring the genetic landscape of Wilms tumor. *Nat. Genet.* **2017**, *49*, 1487−1494.
(24) Perlman, E. J.; Gadd, S.; Arold, S. T.; Radhakrishnan, A.; Gerhard, D. S.; Jennings, L.; Huff, V.; Guidry Auvil, J. M.; Davidsen, T. M.; Dome, J. S.; Meerzaman, D.; Hsu, C. H.; Nguyen, C.; Anderson, J.; Ma, Y.; Mungall, A. J.; Moore, R. A.; Marra, M. A.; Mullighan, C. G.; Ma, J.; Wheeler, D. A.; Hampton, O. A.; Gastier-Foster, J. M.; Ross, N.; Smith, M. A. MLLT1 YEATS domain mutations in clinically distinctive Favourable Histology Wilms tumours. *Nat. Commun.* **2015**, *6*, 10013.
(25) Wan, L.; Chong, S.; Xuan, F.; Liang, A.; Cui, X.; Gates, L.; Carroll, T. S.; Li, Y.; Feng, L.; Chen, G.; Wang, S.-P.; Ortiz, M. V.; Daley, S. K.; Wang, X.; Xuan, H.; Kentsis, A.; Muir, T. W.; Roeder, R. G.; Li, H.; Li, W.; Tjian, R.; Wen, H.; Allis, C. D. Impaired cell fate through gain-of-function mutations in a chromatin reader. *Nature* **2020**, *577*, 121−126.
(26) Asiaban, J. N.; Milosevich, N.; Chen, E.; Bishop, T. R.; Wang, J.; Zhang, Y.; Ackerman, C. J.; Hampton, E. N.; Young, T. S.; Hull, M. V.; Cravatt, B. F.; Erb, M. A. Cell-Based ligand discovery for the ENL YEATS domain. *ACS Chem. Biol.* **2020**, *15*, 895−903.
(27) Christott, T.; Bennett, J.; Coxon, C.; Monteiro, O.; Giroud, C.; Beke, V.; Felce, S. L.; Gamble, V.; Gileadi, C.; Poda, G.; Al-Awar, R.; Farnie, G.; Fedorov, O. Discovery of a selective inhibitor for the YEATS domains of ENL/AF9. *SLAS Discovery* **2019**, *24*, 133−141.
(28) Heidenreich, D.; Moustakim, M.; Schmidt, J.; Merk, D.; Brennan, P. E.; Fedorov, O.; Chaikuad, A.; Knapp, S. Structure-based approach toward identification of inhibitory fragments for Eleven-Nineteen-Leukemia Protein (ENL). *J. Med. Chem.* **2018**, *61*, 10929−10934.
(29) Jiang, Y.; Chen, G.; Li, X.-M.; Liu, S.; Tian, G.; Li, Y.; Li, X.; Li, H.; Li, X. D. Selective targeting of AF9 YEATS domain by cyclopeptide inhibitors with preorganized conformation. *J. Am. Chem. Soc.* **2020**, *142*, 21450−21459.
(30) Li, X.; Li, X.-M.; Jiang, Y.; Liu, Z.; Cui, Y.; Fung, K. Y.; van der Beelen, S. H. E.; Tian, G.; Wan, L.; Shi, X.; Allis, C. D.; Li, H.; Li, Y.; Li, X. D. Structure-guided development of YEATS domain inhibitors by targeting pi-pi-pi stacking. *Nat. Chem. Biol.* **2018**, *14*, 1140−1149.
(31) Moustakim, M.; Christott, T.; Monteiro, O. P.; Bennett, J.; Giroud, C.; Ward, J.; Rogers, C. M.; Smith, P.; Panagakou, I.; Díaz-Sáez, L.; Felce, S. L.; Gamble, V.; Gileadi, C.; Halidi, N.; Heidenreich, D.; Chaikuad, A.; Knapp, S.; Huber, K. V. M.; Farnie, G.; Heer, J.; Manevski, N.; Poda, G.; Al-Awar, R.; Dixon, D. J.; Brennan, P. E.; Fedorov, O. Discovery of an MLLT1/3 YEATS domain chemical probe. *Angew. Chem., Int. Ed.* **2018**, *57*, 16302−16307.
(32) Ni, X.; Heidenreich, D.; Christott, T.; Bennett, J.; Moustakim, M.; Brennan, P. E.; Fedorov, O.; Knapp, S.; Chaikuad, A. Structural insights into interaction mechanisms of alternative piperazine-urea YEATS domain binders in MLLT1. *ACS Med. Chem. Lett.* **2019**, *10*, 1661−1666.
(33) Klein, B. J.; Piao, L.; Xi, Y.; Rincon-Arano, H.; Rothbart, S. B.; Peng, D.; Wen, H.; Larson, C.; Zhang, X.; Zheng, X.; Cortazar, M. A.; Peña, P. V.; Mangan, A.; Bentley, D. L.; Strahl, B. D.; Groudine, M.; Li, W.; Shi, X.; Kutateladze, T. G. The histone-H3K4-specific demethylase KDM5B binds to its substrate and product through distinct PHD fingers. *Cell Rep.* **2014**, *6*, 325−335.
(34) Jafari, R.; Almqvist, H.; Axelsson, H.; Ignatushchenko, M.; Lundbäck, T.; Nordlund, P.; Molina, D. M. The cellular thermal shift assay for evaluating drug target interactions in cells. *Nat. Protoc.* **2014**, *9*, 2100−2122.
(35) Di Veroli, G. Y.; Fornari, C.; Wang, D.; Mollard, S.; Bramhall, J. L.; Richards, F. M.; Jodrell, D. I. Combenefit: an interactive platform for the analysis and visualization of drug combinations. *Bioinformatics* **2016**, *32*, 2866−2868.
(36) Fischer, U.; Meltzer, P.; Meese, E. Twelve amplified and expressed genes localized in a single domain in glioma. *Hum. Genet.* **1996**, *98*, 625−628.
(37) Pikor, L. A.; Lockwood, W. W.; Thu, K. L.; Vucic, E. A.; Chari, R.; Gazdar, A. F.; Lam, S.; Lam, W. L. YEATS4 is a novel oncogene amplified in non-small cell lung cancer that regulates the p53 pathway. *Cancer Res.* **2013**, *73*, 7301−7312.
(38) Zimmermann, K.; Ahrens, K.; Matthes, S.; Buerstedde, J.-M.; Strätling, W. H.; Phi-van, L. Targeted disruption of the GAS41 gene encoding a putative transcription factor indicates that GAS41 is essential for cell viability. *J. Biol. Chem.* **2002**, *277*, 18626−18631.
(39) Morris, G. M.; Huey, R.; Lindstrom, W.; Sanner, M. F.; Belew, R. K.; Goodsell, D. S.; Olson, A. J. AutoDock4 and AutoDockTools4: Automated docking with selective receptor flexibility. *J. Comput. Chem.* **2009**, *30*, 2785−2791.

https://doi.org/10.1021/acs.jmedchem.1c00367
J. Med. Chem. XXXX, XXX, XXX−XXX